To appear in: **Mathematical Sciences**

Online ISSN: 2251-7456 Print ISSN: 2008-1359

Received: 20- November-2025

Revised: 24- April-2026

Accepted: 14- May-2026

DOI: https://doi.org/10.57647/mathsci.89bj.w891

ORIGINAL RESEARCH

A robust Galerkin fractional Taylor technique to solve multi-dimensional fractional optimal control problems with inequality constraints

Lakhlifa Sadek[1,2], Ibtisam Aldawish[3,*], Zakia Hammouch[4,5,†]
Ahmad Shafee[6,] and Ioan-Lucian Popa[7,8]

[1]Department of Mathematics, Saveetha School of Engineering,
Saveetha Institute of Medical and Technical Sciences,
Chennai 602105, Tamilnadu, India
l.sadek@uae.ac.ma
[2]Department of Mathematics, Faculty of Sciences and Technology, Al-Hoceima,
Abdelmalek Essaadi University, Tetouan, Morocco
ORCID: 0000-0001-9780-2592
[3]Department of Mathematics and Statistics, College of Science,
Imam Mohammad Ibn Saud Islamic University (IMSIU), Riyadh, Saudi Arabia
imaldawish@imamu.edu.sa
ORCID: 0000-0003-0745-3347
[4]Department of Medical Research,
China Medical University Hospital, Taichung, Taiwan
[5]Department of Mathematics, Kyung Hee University, 26 Kyungheedae-Ro,
Dongdaemun-Gu, Seoul, 02447, South Korea
hammouch_Zakia@tdmu.edu.vn
[6]Laboratory Technology Department , College of Technological Studies,
Public Authority for Applied Education and Training (PAAET), Shuwaikh, Kuwait
as.zada@paaet.edu.kw
[7]Department of Computing, Mathematics and Electronics,
"1 Decembrie 1918" University of Alba Iulia, 510009, Alba Iulia, Romania
[8]Faculty of Mathematics and Computer Science,
Transilvania University of Brasov, Iuliu Maniu Street 50, 500091, Brasov, Romania
lucian.popa@uab.ro

May 28, 2026

Abstract

A new computational approach is presented for solving MFOCPs subject to Caputo fractional dynamics by means of Galerkin projection technique along with fractional Taylor polynomial expansions. The method successfully deals with constraints in the form of both equalities and inequalities. An important feature of the new method

*Corresponding author: imaldawish@imamu.edu.sa
†Corresponding author: hammouch_Zakia@tdmu.edu.vn

includes deriving an operational matrix based on fractional Taylor polynomials such that, using the Galerkin approach, the problem under study is reduced to a set of algebraic equations. Convergence analysis of the Taylor series expansions is investigated in detail. The performance of the approach is confirmed by applying it to four problems in comparison with other existing approaches in the literature.

Keywords: MFOCPs; Caputo fractional derivative (CFD); Riemann-Liouville fractional integral (RLI); fractional Taylor polynomials; Galerkin method; error estimation.

MSC 2010: 49M05; 65T60.

1 Introduction

The topic of optimal control is of great importance in different fields within engineering, as well as computational science. This theory allows solving mathematical problems associated with developing optimal controls, either minimizing cost functionals or maximizing some criteria for dynamical processes [1]. Despite being quite established, a prominent modern generalization of optimal control problems is the inclusion of these optimization problems within the realm of fractional calculus. Here, the MFOCP framework transcends the classical theory of control ($\varrho = 1$) to accommodate dynamic systems described by FDE [2, 3]. The use of fractional calculus in modeling such systems is a rather modern concept that allows for the modeling of hereditary dynamical systems [4].

Applications of MFOCPs are wide-ranging and found across many different areas of engineering. Examples include the study of nonlinear vibrations of the Van der Pol oscillator [5], the control of feedback linearizable systems [6], the well-known Breakwell problem [7], and accurate operation of human-controlled crane bridges [8]. There has been increasing attention paid to this topic, resulting in some recent publications on the theory and numerical solution of MFOCPs [9–11]. For example, recent research has been conducted on the finite-time synchronization of fractional-order fuzzy neural networks with nonlinear feedback control [12] and with discrete-time approaches [13]. Moreover, there have been numerical techniques, such as the extended truncated exponential technique, designed to solve these difficult problems [14].

One important category of direct methods is those where the original problem is transformed to a finite-dimensional nonlinear programming problem via parameterization. One popular and efficient method belonging to this class is spectral methods. In this method, the solution is approximated using a family of orthogonal functions or polynomials. The success of this method depends on the selection of these basis functions. Several investigations have been carried out using various basis functions and some of these include: Chebyshev [15, 16], Bernoulli [17], Legendre [2], Hermite [4], Bell Polynomials [18], Haar Wavelets [19], Legendre Wavelets [20], Block Pulse functions [1], Pell-Lucas Polynomials [21] and Mittag-Leffler Function [22]. This body of work demonstrates that the choice of basis functions is critical, influencing the accuracy, convergence rate, and computational efficiency of the resulting algorithm.

Indeed, the design of accurate numerical schemes for fractional and integral equations is still being investigated extensively by researchers, and several current contributions are showing the focus of the researcher on spectral order and convergence. This is consistent with an emerging trend that takes advantage of the efficiency of the spectral and pseudo-spectral Galerkin approach to generate an accurate solution. For example, current contributions have

used the Legendre pseudo-spectral element method [23] and the multistep pseudo-spectral continuous Galerkin scheme [24] in the solution of Volterra integro-differential equations. This emphasis on achieving maximum accuracy is even more apparent from the resolution of high-order nonlinear [25] and weakly singular [26] differential equations, where spectral Galerkin schemes have proven to be extremely successful. Within the particular area of fractional optimal control, which has functional similarities with the previous categories of differential equations, one finds that the quest for efficient basis functions remains an important objective, as demonstrated by recent studies whose main objective was increased efficiency and precision [27]. Our new GFT methodology plays its role in this continued endeavor through developing a special type of fractional polynomial basis function within the context of Galerkin projection schemes, particularly for multi-dimensional fractional optimal control systems involving inequality constraints.

The fractional Taylor polynomials offer several distinct advantages for solving MFOCPs. First, their monomial structure $\mathcal{T}_i(x) = x^{i\rho}$ naturally aligns with the power-law behavior inherent in fractional calculus, enabling exact representation of fractional integrals via the operational matrix derived in Section 5. Second, the basis functions are orthogonalizable on $[0, 1]$ with respect to the standard $\mathbb{L}^2$ inner product, which facilitates stable numerical computations. Third, unlike classical polynomial bases that require fractional differentiation of the basis functions, the fractional Taylor basis allows direct and exact application of the RL integral operator through simple coefficient scaling. This property significantly reduces computational complexity and improves accuracy. Fourth, the basis provides spectral convergence for sufficiently smooth solutions, as demonstrated in our error analysis (Theorem 2).

The method based on operational matrices, which is well-established in literature for solving several problems related to fractional calculus [28, 29], has the following remarkable features: (i) the fractional calculus operations can be represented in terms of algebraic matrix operations, hence, the computation becomes cheaper; (ii) high-dimensional problems can be solved by taking advantage of Kronecker products; (iii) Galerkin projection in combination with this technique preserves spectral accuracy; and (iv) incorporating initial/boundary conditions becomes more straightforward. In this paper, we introduce a new operational matrix Π^ρ for the fractional integral operator in the sense of Riemann-Liouville using fractional Taylor polynomials. Using this operational matrix, the state functions can be recovered from their fractional derivatives by a simple formula $\mathrm{RL}\mathcal{I}^\rho \mathbb{T}_d(x) \approx \Pi^\rho \mathbb{T}_d(x)$ without any quadrature technique, ensuring exponential convergence rates.

Although Galerkin-fractional Taylor (GFT) has been used to solve a number of different applications, its use for solving MFOCPs involving inequality constraints is quite rare. The main aim of this paper is to bridge this gap through the proposed framework, which will be used for solving the following MFOCP:

The objective is to minimize

$$J = \int_\Lambda \mathbf{A}\big(\varkappa, \mathbf{X}(\varkappa), \mathbf{V}(\varkappa)\big)\mathrm{d}\varkappa, \quad \text{where } \Lambda = [0, 1], \tag{1}$$

subject to the system dynamics governed by the Caputo fractional derivative,

$${}^{\mathrm{C}}\mathcal{D}^{\varrho}_{\varkappa}\mathbf{X}(\varkappa) = \mathbf{B}(\varkappa, \mathbf{X}(\varkappa), \mathbf{V}(\varkappa)), \quad m - 1 \le \varrho < m, \quad \varkappa \in \Lambda, \tag{2}$$

a set of s nonlinear inequality path constraints,

$$\mathbf{C}_i(\varkappa, \mathbf{X}(\varkappa), \mathbf{V}(\varkappa)) \le 0, \quad i = 1, 2, \ldots, s, \tag{3}$$

and the conditions

$$\mathbf{X}^{(i)}(0) = {}_i\mathbf{X}, \quad i = 0, 1, \ldots, m-1. \tag{4}$$

In this formulation, $\mathbf{X}(\varkappa)$ and $\mathbf{V}(\varkappa)$ represent N-dimensional state and control vectors, respectively. The functions $\mathbf{A}$, $\mathbf{B}$, and $\mathbf{C}_i$ are assumed to be smooth and continuously differentiable with respect to their arguments.

The main contribution of this work is a novel methodology that leverages fractional Taylor (FT) polynomial expansions to approximate the solutions to the problem defined by Eqs. (1)–(4). The proposed GFT method transforms the underlying MFOCP into a system of algebraic equations through the application of the Galerkin projection. Solving this resultant system provides an efficient numerical pathway to obtain the approximate optimal state and control trajectories.

The paper is structured in the following way. First of all, in Section 2, we present all required preliminaries regarding fractional calculus and fractional Taylor polynomials. Function approximation theory will be presented in Section 3. In Section 4, we conduct an error analysis for the considered method. The operational matrix for RLI, which plays a crucial role in our approach, will be derived in Section 5. Our novel GFT method will be proposed in Section 6. Finally, a discussion regarding the application of the suggested approach and its performance will be conducted using some numerical examples in Section 7. and a comparative analysis with other methods. We conclude the paper with a summary of results and conclusions in Section 8.

2 Preliminaries and definitions

This section establishes the fundamental definitions and properties from fractional calculus and introduces the fractional Taylor polynomial basis, which are essential for the subsequent development of our method.

2.1 Fractional operators

The CFD and the RLI of order ϱ ($m-1 < \varrho < m$, $m \in \mathbb{N}^*$) for a function $w(\varkappa)$, $\varkappa > 0$, are defined respectively as [30,31]:

$${}^{\mathrm{C}}\mathcal{D}^{\varrho}_{\varkappa} w(\varkappa) = \frac{1}{\Gamma(m-\varrho)} \int_0^{\varkappa} \frac{w^{(m)}(y)}{(\varkappa - y)^{\varrho+1-m}} \mathrm{d}y, \tag{5}$$

and

$${}^{\mathrm{RL}}\mathcal{I}^{\varrho} w(\varkappa) = \frac{1}{\Gamma(\varrho)} \int_0^{\varkappa} (\varkappa - y)^{\varrho-1} w(y) \mathrm{d}y, \tag{6}$$

where $\Gamma(\cdot)$ denotes the Gamma function.

2.2 Essential properties

The following properties of these operators for power functions are crucial [30,31]:

$${}^{\mathrm{C}}\mathcal{D}^{\varrho} \varkappa^{\beta} = \frac{\Gamma(\beta+1)}{\Gamma(\beta+1-\varrho)} \varkappa^{\beta-\varrho}, \qquad {}^{\mathrm{RL}}\mathcal{I}^{\varrho}_{\varkappa} \varkappa^{\beta} = \frac{\Gamma(\beta+1)}{\Gamma(\beta+1+\varrho)} \varkappa^{\beta+\varrho}. \tag{7}$$

Furthermore, these operators satisfy the following fundamental identities:

$$ {}^{\mathrm{C}}\mathcal{D}^{\varrho}\left({}^{\mathrm{RL}}\mathcal{I}^{\varrho}w(\varkappa)\right) = w(\varkappa); \tag{8} $$

$$ {}^{\mathrm{RL}}\mathcal{I}^{\varrho}\left({}^{\mathrm{C}}\mathcal{D}^{\varrho}w(\varkappa)\right) = w(\varkappa) - \sum_{i=0}^{m-1} w^{(i)}(0^{+})\frac{\varkappa^{i}}{i!}; \tag{9} $$

$$ {}^{\mathrm{RL}}\mathcal{I}^{\varrho}\left({}^{\mathrm{RL}}\mathcal{I}^{\beta}w(\varkappa)\right) = {}^{\mathrm{RL}}\mathcal{I}^{\varrho+\beta}w(\varkappa), \quad \beta > 0. \tag{10} $$

2.3 Fractional Taylor polynomials

The fractional Taylor (FT) polynomial of integer degree i is defined as the monomial

$$ \mathcal{T}_{i}(\varkappa) = \varkappa^{i\varrho}, \qquad \varkappa \in \mathbb{R}. \tag{11} $$

A direct application of the property in (7) allows for the exact calculation of the fractional integral of any fractional Taylor polynomial

$$ {}^{\mathrm{RL}}\mathcal{I}^{\varrho}\mathcal{T}_{i}(\varkappa) = {}^{\mathrm{RL}}\mathcal{I}^{\varrho}\varkappa^{i\varrho} = \frac{\Gamma(i\varrho+1)}{\Gamma(i\varrho+1+\varrho)}\varkappa^{i\varrho+\varrho}, \qquad \varkappa \in \mathbb{R}. \tag{12} $$

This property is the cornerstone for constructing the operational matrix of fractional integration.

3 Function approximation

This section details the methodology for approximating functions using fractional Taylor polynomials within the framework of the $\mathbb{L}^{2}(\Lambda)$ Hilbert space.

3.1 Mathematical framework

Let $\mathbb{L}^{2}(\Lambda)$ denote the space of Lebesgue square-integrable functions on the interval $\Lambda = [0, 1]$, equipped with the inner product and norm defined by

$$ \langle y, g\rangle = \int_{\Lambda} y(\varkappa)g(\varkappa)\mathrm{d}\varkappa, \quad \|y\|_{\mathbb{L}} = \sqrt{\langle y, y\rangle}. $$

Consider the finite-dimensional subspace $\mathscr{Y}_{d} \subset \mathbb{L}^{2}(\Lambda)$ spanned by

$$ \mathscr{Y}_{d} = \operatorname{span}\left\{\mathcal{T}_{0}, \mathcal{T}_{1}, \ldots, \mathcal{T}_{d}\right\}. $$

Since $\mathscr{Y}_{d}$ is finite-dimensional, it is closed and complete. Consequently, for any function $h \in \mathbb{L}^{2}(\Lambda)$, there exists a unique best approximation $h_{0} \in \mathscr{Y}_{d}$ that satisfies the orthogonality condition

$$ \langle h - h_{0}, g\rangle = 0, \quad \forall g \in \mathscr{Y}_{d}. \tag{13} $$

This function h_{0} minimizes the distance to h over the subspace

$$ \|h - h_{0}\|_{\mathbb{L}} = \inf_{g\in\mathscr{Y}_{d}} \|h - g\|_{\mathbb{L}}. \tag{14} $$

3.2 Series expansion and coefficient calculation

The best approximation h_0 can be expressed as a linear combination of the basis polynomials

$$h(\varkappa) \simeq h_0(\varkappa) = \sum_{\nu=0}^{d} c_\nu \mathcal{T}_\nu(\varkappa) = \mathbf{C}^T \mathbb{T}_d(\varkappa), \tag{15}$$

where the coefficient vector $\mathbf{C}$ and the basis vector $\mathbb{T}_d$ are given by

$$\mathbf{C} = [c_0, c_1, \ldots, c_d]^T, \qquad \mathbb{T}_d(\varkappa) = [\mathcal{T}_0(\varkappa), \mathcal{T}_1(\varkappa), \ldots, \mathcal{T}_d(\varkappa)]^T.$$

To determine the coefficients $\mathbf{C}$, we enforce the orthogonality condition (13). Defining the moments of h as

$$k_i = \langle h(\varkappa), \mathcal{T}_i(\varkappa) \rangle = \int_0^1 h(\varkappa)\mathcal{T}_i(\varkappa)\mathrm{d}\varkappa, \quad i = 0, 1, \ldots, d,$$

and substituting the expansion (15) yields

$$\begin{aligned} k_i &= \int_0^1 \left(\sum_{\nu=0}^{d} c_\nu \mathcal{T}_\nu(\varkappa) \right) \mathcal{T}_i(\varkappa)\mathrm{d}\varkappa \\ &= \sum_{\nu=0}^{d} c_\nu \int_0^1 \mathcal{T}_\nu(\varkappa)\mathcal{T}_i(\varkappa)\mathrm{d}\varkappa = \sum_{\nu=0}^{d} c_\nu \, r_{\nu i}, \end{aligned} \tag{16}$$

where $r_{\nu i} = \langle \mathcal{T}_\nu, \mathcal{T}_i \rangle$. Letting $\mathbf{K} = [k_0, k_1, \ldots, k_d]^T$ and $\mathbf{R} = [r_{\nu i}]_{(d+1)\times(d+1)}$, the system in (16) can be written in matrix form as

$$\mathbf{K} = \mathbf{R}\,\mathbf{C}. \tag{17}$$

The entries of the matrix $\mathbf{R}$ are easily computed, we have

$$r_{\nu i} = \langle \mathcal{T}_\nu, \mathcal{T}_i \rangle = \int_0^1 \varkappa^{\nu\varrho}\varkappa^{i\varrho}\mathrm{d}\varkappa = \int_0^1 \varkappa^{\nu\varrho + i\varrho}\mathrm{d}\varkappa = \frac{1}{\nu\varrho + i\varrho + 1}.$$

Thus, $\mathbf{R}$ is a well-known Hilbert-like matrix. The coefficient vector is then obtained by solving the linear system

$$\mathbf{C} = \mathbf{R}^{-1}\mathbf{K}.$$

Therefore, the best approximation of any function $h \in \mathbb{L}^2(\Lambda)$ in the $\mathbb{L}^2$-norm is given by

$$h(\varkappa) \simeq \mathbf{C}^T \mathbb{T}_d(\varkappa) = \mathbf{K}^T \mathbf{R}^{-1} \mathbb{T}_d(\varkappa). \tag{18}$$

3.3 Linear independence and completeness

The linear independence of the set $\{\mathcal{T}_0, \mathcal{T}_1, \ldots, \mathcal{T}_d\}$ is evident from the fundamental theorem of algebra: if a linear combination of these distinct monomials is identically zero, then all coefficients must be zero. This property, combined with the existence and uniqueness of the best approximation (14), confirms that the fractional Taylor polynomials form a complete basis for the finite-dimensional subspace $\mathscr{Y}_d$.

4 Error and convergence analysis

This section provides a theoretical analysis of the error incurred by the fractional Taylor polynomial approximation and establishes the framework for a posteriori error estimation for the MFOCP.

4.1 Approximation error bound

Assumption 4.1 (Solution Regularity). The exact solution functions $\mathbf{X}(\varkappa)$ and $\mathbf{V}(\varkappa)$ are assumed to be $(d+1)$-times continuously differentiable on $\Lambda = [0,1]$, and their fractional derivatives ${}^{C}\mathcal{D}^{(d+1)\varrho}\mathbf{X}(\varkappa)$, ${}^{C}\mathcal{D}^{(d+1)\varrho}\mathbf{V}(\varkappa)$ exist and are continuous.

We begin by establishing a bound on the error of the best approximation in the $\mathbb{L}^2$ norm.

Theorem 1. *[32] Suppose that* ${}^{\mathrm{C}}\mathcal{D}^{k\varrho}_{\varkappa} y(\varkappa) \in C(0,b]$ *for* $k = 0, 1, \ldots, m+1$, *where* $0 < \varrho \leqslant 1$, *then we have*

$$y(\varkappa) = \sum_{i=0}^{m} \frac{\varkappa^{i\varrho}}{\Gamma(i\varrho+1)} \left({}^{\mathrm{C}}\mathcal{D}^{i\varrho}_{\varkappa} y\right)(0) + \frac{\left({}^{\mathrm{C}}\mathcal{D}^{(m+1)\varrho} y\right)(\xi)}{\Gamma((m+1)\varrho+1)} \varkappa^{(m+1)\varrho},$$

with $0 \leqslant \xi \leqslant \varkappa, \forall \varkappa \in (0,b]$, *where*

$${}^{\mathrm{C}}\mathcal{D}^{m\varrho} = {}^{\mathrm{C}}\mathcal{D}^{\varrho} \,.\, {}^{\mathrm{C}}\mathcal{D}^{\varrho} \ldots {}^{\mathrm{C}}\mathcal{D}^{\varrho} \quad (m\text{-}times).$$

Theorem 2. *Let* $w \in C^{d+1}(\Lambda)$ *be a* $(d+1)$*-times continuously differentiable function (satisfying Assumption 4.1) and let* $\mathscr{U}_d = \operatorname{span}\{\mathcal{T}_0, \mathcal{T}_1, \ldots, \mathcal{T}_d\}$ *be the space of Taylor polynomials of degree at most* d. *Let* ${}^{d}w \in \mathscr{U}_d$ *be the best approximation of* w *in the* $\mathbb{L}^2(\Lambda)$ *norm. Then, under the regularity conditions of Assumption 4.1, the approximation error is bounded by:*

$$\left\| w - {}^{d}w \right\|_{\mathbb{L}} \leq \frac{\delta}{\Gamma((d+1)\varrho+1)\sqrt{2d\varrho+2\varrho+1}}, \qquad \text{where} \quad \delta = \max_{\varkappa\in\Lambda} \left| \left({}^{C}\mathcal{D}^{(d+1)\varrho} w\right)(\varkappa) \right|.$$

Proof. We start by constructing the fractional Taylor polynomial $\hat{y}_1(\varkappa) \in \mathscr{Y}_d$ expanded around $\varkappa = 0$:

$$\hat{y}_1(\varkappa) = \sum_{i=0}^{d} \frac{\varkappa^{i\varrho}}{\Gamma(i\varrho+1)} \left({}^{\mathrm{C}}\mathcal{D}^{i\varrho}_{\varkappa} w\right)(0).$$

Applying the generalized Taylor theorem (Theorem 1), for each $\varkappa \in \Lambda$ there exists a point $\xi_\varkappa \in (0,\varkappa)$ such that the remainder satisfies

$$|w(\varkappa) - \hat{y}_1(\varkappa)| = \left| \frac{\left({}^{\mathrm{C}}\mathcal{D}^{(d+1)\varrho} w\right)(\xi)}{\Gamma((d+1)\varrho+1)} \varkappa^{(d+1)\varrho} \right| \leq \frac{\delta\, \varkappa^{(d+1)\varrho}}{\Gamma((d+1)\varrho+1)}. \tag{19}$$

Since ${}^{d}w$ is the best approximation of w in $\mathscr{Y}_d$ and $\hat{y}_1 \in \mathscr{Y}_d$, it follows from the definition of the best approximation that:

$$\left\| w - {}^{d}w \right\|^2_{\mathbb{L}} \leq \|w - \hat{y}_1\|^2_{\mathbb{L}}\,.$$

Using the pointwise bound, we estimate this norm, we have

$$\begin{aligned}\|w-\hat{y}_1\|_{\mathbb{L}}^2 &= \int_0^1 |w(\varkappa)-\hat{y}_1(\varkappa)|^2\,\mathrm{d}\varkappa \\ &\leq \int_0^1 \left(\frac{\delta\,\varkappa^{(d+1)\varrho}}{\Gamma((d+1)\varrho+1)}\right)^2 \mathrm{d}\varkappa \\ &= \left(\frac{\delta}{\Gamma((d+1)\varrho+1)}\right)^2 \int_0^1 \varkappa^{2d\varrho+2\varrho}\mathrm{d}\varkappa \\ &= \frac{\delta^2}{\left(\Gamma((d+1)\varrho+1)\right)^2(2d\varrho+2\varrho+1)}.\end{aligned}$$

Taking the square root of both sides yields the desired result

$$\left\|w-{}^{d}w\right\|_{\mathbb{L}} \leq \frac{\delta}{\Gamma((d+1)\varrho+1)\sqrt{2d\varrho+2\varrho+1}}.$$

□

4.2 A posteriori error estimation for the MFOCP

The following theorem formalizes the error dynamics for the MFOCP, providing a framework for a posteriori error analysis.

Theorem 3. *Let (V_1, V_2) be the exact state and control functions satisfying the MFOCP (1)–(4). Let $({}^{d}V_1, {}^{d}V_2)$ be their approximations obtained by the GFT method. Then, the approximation errors ${}^{d}\mathbb{E}^{V_i}(\varkappa) = V_i(\varkappa) - {}^{d}V_i(\varkappa)$, for $i = 1, 2$, satisfy the following MFOCP:*

$$\min J_d = \int_0^1 \mathbf{A}\left(\varkappa, {}^{d}\mathbb{E}^{V_1}(\varkappa) + {}^{d}V_1(\varkappa), {}^{d}\mathbb{E}^{V_2}(\varkappa) + {}^{d}V_2(\varkappa)\right)\mathrm{d}\varkappa, \tag{20}$$

subject to

$${}^{\mathrm{C}}\mathcal{D}_{\varkappa}^{\varrho}\left({}^{d}\mathbb{E}^{V_1}(\varkappa) + {}^{d}V_1(\varkappa)\right) = \mathbf{B}\left(\varkappa, {}^{d}\mathbb{E}^{V_1}(\varkappa) + {}^{d}V_1(\varkappa), {}^{d}\mathbb{E}^{V_2}(\varkappa) + {}^{d}V_2(\varkappa)\right), \tag{21}$$

$$\mathbf{C}_j\left(\varkappa, {}^{d}\mathbb{E}^{V_1}(\varkappa) + {}^{d}V_1(\varkappa), {}^{d}\mathbb{E}^{V_2}(\varkappa) + {}^{d}V_2(\varkappa)\right) \leq 0, \quad j = 1, \ldots, s, \tag{22}$$

and initial conditions (23)

$$\left({}^{d}\mathbb{E}^{V_1}\right)^{(k)}(0) = {}_{k}V_1 - {}^{d}V_1^{(k)}(0), \quad k = 0, 1, \ldots, m-1.$$

Proof. The result follows directly from the linearity of the Caputo derivative and the initial conditions, by substituting $V_i(\varkappa) = {}^{d}\mathbb{E}^{V_i}(\varkappa) + {}^{d}V_i(\varkappa)$, for $i = 1, 2$, into the original problem (1)–(4). □

Practical implementation: The error MFOCP (20)–(23) is solved using the same GFT method with the same basis functions $\{\mathcal{T}_i(\varkappa)\}$, but typically with a higher polynomial degree $d' > d$. This allows for a more accurate representation of the error functions ${}^{d'}\mathbb{E}^{\mathbf{X}}(\varkappa)$ and ${}^{d'}\mathbb{E}^{\mathbf{V}}(\varkappa)$.

4.3 Iterative error correction

As Theorem 3 indicates, the error functions ${}^{d}\mathbb{E}^{\mathbf{X}}$ and ${}^{d}\mathbb{E}^{\mathbf{V}}$ can also be regarded as solutions of another MFOCP. This indicates an iterative improvement process whereby the GFT algorithm is used for solving the error MFOCP Eqs. (20)–(23) to obtain a further approximation of the error.

Let ${}^{d',d}\mathbb{E}^{j}(\varkappa)$, $j = 1, 2$, be the approximate solutions for the error functions obtained by applying the GFT method with a new, higher polynomial degree d' to the system (20)–(23). The corrected solution is then given by:

$$
\begin{aligned}
{}^{d'}\mathbf{X}_{\text{corrected}}(\varkappa) &= {}^{d}\mathbf{X}(\varkappa) + {}^{d',d}\mathbb{E}^{\mathbf{X}}(\varkappa),\\
{}^{d'}\mathbf{V}_{\text{corrected}}(\varkappa) &= {}^{d}\mathbf{V}(\varkappa) + {}^{d',d}\mathbb{E}^{\mathbf{V}}(\varkappa).
\end{aligned}
$$

In fact, one can increase the polynomial order dynamically with respect to the size of the approximate error. For example, if one starts from a polynomial order d_0 and if the norm of the approximate error $\|{}^{d',d}\mathbb{E}\|$ exceeds some threshold value ϵ_{tol}, then the polynomial order d' will be higher than d. In such cases, the MFOCP error should be resolved again. This method provides a way to perform a posteriori error estimation, which is especially useful in situations where no expression of the exact solution is available.

5 Operational matrix for the RLI

This section is dedicated to the derivation of the operational matrix for the RLI, which is a crucial component for the numerical implementation of our method.

5.1 Derivation of the matrix

The goal is to find a matrix $\mathbf{\Pi}^{\varrho}$ such that the RLI of the fractional Taylor basis vector can be expressed as

$$
{}^{\mathrm{RL}}\mathcal{I}^{\varrho}\mathbb{T}_d(\varkappa) \approx \mathbf{\Pi}^{\varrho}\,\mathbb{T}_d(\varkappa), \tag{24}
$$

where $\mathbb{T}_d(\varkappa) = [1, \varkappa^{\varrho}, \varkappa^{2\varrho}, \ldots, \varkappa^{d\varrho}]^T$.

We begin by applying the RLI operator to each element of the basis vector. Using the known formula for the RLI of a power function from Eq. (7), we obtain

$$
\begin{aligned}
{}^{\mathrm{RL}}\mathcal{I}^{\varrho}\mathbb{T}_d(\varkappa) &= \left[{}^{\mathrm{RL}}\mathcal{I}^{\varrho}(1), {}^{\mathrm{RL}}\mathcal{I}^{\varrho}(\varkappa^{\varrho}), \ldots, {}^{\mathrm{RL}}\mathcal{I}^{\varrho}(\varkappa^{d\varrho})\right]^T\\
&= \left[\frac{\Gamma(1)}{\Gamma(1+\varrho)}\varkappa^{\varrho}, \frac{\Gamma(\varrho+1)}{\Gamma(\varrho+1+\varrho)}\varkappa^{2\varrho}, \ldots, \frac{\Gamma(d\varrho+1)}{\Gamma(d\varrho+1+\varrho)}\varkappa^{d\varrho+\varrho}\right]^T.
\end{aligned} \tag{25}
$$

This result can be written compactly as

$$
{}^{\mathrm{RL}}\mathcal{I}^{\varrho}\mathbb{T}_d(\varkappa) = \mathbf{\Omega}\,\boldsymbol{\vartheta}(\varkappa), \tag{26}
$$

where $\mathbf{\Omega}$ is a diagonal matrix of coefficients and $\boldsymbol{\vartheta}(\varkappa)$ is a vector of shifted monomials

$$
\mathbf{\Omega} = \operatorname{diag}\left(\frac{\Gamma(1)}{\Gamma(1+\varrho)}, \frac{\Gamma(\varrho+1)}{\Gamma(\varrho+1+\varrho)}, \ldots, \frac{\Gamma(d\varrho+1)}{\Gamma(d\varrho+1+\varrho)}\right), \quad \boldsymbol{\vartheta}(\varkappa) = \left[\varkappa^{\varrho}, \varkappa^{2\varrho}, \ldots, \varkappa^{\varrho+d\varrho}\right]^T.
$$

5.2 Projection onto the fractional Taylor basis

The vector $\boldsymbol{\vartheta}(\varkappa)$ lies outside the original polynomial space $\mathscr{Y}_d$ due to the non-integer exponent ϱ. To express it in terms of the basis $\mathbb{T}_d(\varkappa)$, we project each component $\varkappa^{\varrho+i\varrho}$ onto $\mathscr{Y}_d$. From the approximation theory in Section 3, specifically Eq. (18), we have:

$$\varkappa^{\varrho+i\varrho} \approx \mathbf{P}_i\, \mathbb{T}_d(\varkappa), \quad \text{for } i = 0, 1, \ldots, d, \tag{27}$$

where the row vector $\mathbf{P}_i$ contains the expansion coefficients for $\varkappa^{\varrho+i\varrho}$. These coefficients are found by solving the linear system derived from the inner products

$$\mathbf{P}_i = \overline{\mathbf{P}}_i\, \mathbf{R}^{-1}.$$

Here, $\mathbf{R}$ is the Gram matrix defined in Section 3, and the vector $\overline{\mathbf{P}}_i$ is given by

$$\overline{\mathbf{P}}_i = \left[\langle \varkappa^{\varrho+i\varrho}, \mathcal{T}_0\rangle, \langle \varkappa^{\varrho+i\varrho}, \mathcal{T}_1\rangle, \ldots, \langle \varkappa^{\varrho+i\varrho}, \mathcal{T}_d\rangle\right] = \left[\int_0^1 \varkappa^{\varrho+i\varrho+j\varrho}\mathrm{d}\varkappa\right]_{j=0}^{d} = \left[\frac{1}{\varrho+i\varrho+j\varrho+1}\right]_{j=0}^{d}.$$

Assembling the approximations for all i into a single matrix equation, we can write

$$\boldsymbol{\vartheta}(\varkappa) = \begin{bmatrix} \varkappa^{\varrho} \\ \varkappa^{2\varrho} \\ \vdots \\ \varkappa^{\varrho+d\varrho} \end{bmatrix} \approx \begin{bmatrix} \mathbf{P}_0 \\ \mathbf{P}_1 \\ \vdots \\ \mathbf{P}_d \end{bmatrix} \mathbb{T}_d(\varkappa) = \begin{bmatrix} \overline{\mathbf{P}}_0\mathbf{R}^{-1} \\ \overline{\mathbf{P}}_1\mathbf{R}^{-1} \\ \vdots \\ \overline{\mathbf{P}}_d\mathbf{R}^{-1} \end{bmatrix} \mathbb{T}_d(\varkappa). \tag{28}$$

The block matrix in Eq. (28) is a diagonal matrix of row vectors. Its structure can be represented as

$$\boldsymbol{\vartheta}(\varkappa) \approx \mathbf{P}\, (\mathbf{1} \otimes \mathbb{T}_d(\varkappa)),$$

where $\mathbf{1}$ is a column vector of ones of length $(d+1)$, $\otimes$ denotes the Kronecker product, and $\mathbf{P}$ is the block diagonal matrix

$$\mathbf{P} = \text{blockdiag}\left(\overline{\mathbf{P}}_0\mathbf{R}^{-1}, \overline{\mathbf{P}}_1\mathbf{R}^{-1}, \ldots, \overline{\mathbf{P}}_d\mathbf{R}^{-1}\right).$$

5.3 Final operational matrix form

Substituting the approximation from Eq. (28) into Eq. (26) yields the final form of the operational matrix:

$$\begin{aligned} {}^{\mathrm{RL}}\mathcal{I}^{\varrho}\mathbb{T}_d(\varkappa) &\approx \boldsymbol{\Omega}\,\mathbf{P}\, (\mathbf{1} \otimes \mathbb{T}_d(\varkappa)) \\ &= \underbrace{\boldsymbol{\Omega}\,\mathbf{P}}_{\boldsymbol{\Pi}^{\varrho}} (\mathbf{1} \otimes \mathbb{T}_d(\varkappa)). \end{aligned} \tag{29}$$

The matrix $\boldsymbol{\Pi}^{\varrho} = \boldsymbol{\Omega}\,\mathbf{P}$ is the desired $(d+1) \times (d+1)$ operational matrix of fractional integration for the fractional Taylor basis. This matrix allows us to efficiently compute the fractional integral of any function expressed in the fractional Taylor polynomial basis by performing a simple matrix-vector multiplication.

6 Description of the GFT method

This section details the application of the GFT method to solve the MFOCP with inequality constraints as defined in Eqs. (1)–(4). The core idea is to approximate the state and control variables using fractional Taylor polynomial expansions and then employ the Galerkin projection to transform the original problem into a system of algebraic equations.

Using the theoretical results developed in Sections 2–5, the following is a summary of the entire computational process of using the GFT approach. The following algorithm describes the entire process from the initialization of the coefficients matrices to obtaining the optimum state and control trajectories. This algorithm makes use of the Galerkin approximation, the operational matrix of fractional integration found in Section 5, and the Newton iteration scheme.

6.1 Polynomial approximation of variables

In this subsection, we commence by expressing the CFD of the state vector and the control vector themselves as expansions in the fractional Taylor polynomial basis $\mathbb{T}_d(\varkappa)$:

$$ {}^{\mathrm{C}}\mathcal{D}_{\varkappa}^{\varrho\, d} X_i(\varkappa) = \mathbf{T}^i\, \mathbb{T}_d(\varkappa), \quad \text{where} \quad \mathbf{T}^i = [T_0^i, T_1^i, \ldots, T_d^i], \tag{30} $$

$$ {}^{d}V_j(\varkappa) = \mathbf{U}^j \mathbb{T}_d(\varkappa), \quad \text{where} \quad \mathbf{U}^j = [u_0^j, u_1^j, \ldots, u_d^j], \tag{31} $$

for $i, j = 1, 2, \ldots, N$. Here, ${}^{d}X_i$ and ${}^{d}V_j$ denote the d-th order approximations of the state and control components, respectively.

These component-wise approximations can be assembled into compact vector-matrix forms for the entire system:

$$ {}^{\mathrm{C}}\mathcal{D}_{\varkappa}^{\varrho\, d}\mathbf{X}(\varkappa) = \left(\mathbf{I}_N \otimes \mathbb{T}_d(\varkappa)^T\right) \widehat{\mathbf{T}}^T, \tag{32} $$

$$ {}^{d}\mathbf{V}(\varkappa) = \left(\mathbf{I}_N \otimes \mathbb{T}_d(\varkappa)^T\right) \widehat{\mathbf{U}}^T, \tag{33} $$

where $\mathbf{I}_N$ is the $N \times N$ identity matrix, $\otimes$ denotes the Kronecker product, and the aggregate coefficient matrices are defined as:

$$ \widehat{\mathbf{U}} = \begin{bmatrix} \mathbf{U}^1 & \mathbf{U}^2 & \ldots & \mathbf{U}^N \end{bmatrix}, \qquad \widehat{\mathbf{T}} = \begin{bmatrix} \mathbf{T}^1 & \mathbf{T}^2 & \ldots & \mathbf{T}^N \end{bmatrix}. \tag{34} $$

6.2 Recovering the state approximation

In order to derive an estimate for the state vector $\mathbf{X}(\varkappa)$, we take the Riemann-Liouville fractional integral of order ϱ on both sides of Eq. (32). From the property of inversion of fractional calculus according to Eq. (9), we have

$$ \begin{aligned} {}^{d}\mathbf{X}(\varkappa) &= {}^{\mathrm{RL}}\mathcal{I}^{\varrho}\left({}^{\mathrm{C}}\mathcal{D}_{\varrho}^{\varrho\, d}\mathbf{X}(\varkappa)\right) + \sum_{k=0}^{n-1} {}_k\mathbf{X}\, \frac{\varkappa^k}{k!} \\ &= {}^{\mathrm{RL}}\mathcal{I}^{\varrho}\left(\left(\mathbf{I}_N \otimes \mathbb{T}_d(\varkappa)^T\right) \widehat{\mathbf{T}}^T\right) + \sum_{k=0}^{n-1} {}_k\mathbf{X} \frac{\varkappa^k}{k!}. \end{aligned} \tag{35} $$

Leveraging the linearity of the integral operator and the operational matrix $\mathbf{\Pi}^{\varrho}$ derived in Section 5 (Eq. (29)), this expression simplifies to

$$ {}^{d}\mathbf{X}(\varkappa) = \mathbf{\Phi}(\varkappa)\, \widehat{\mathbf{T}}^T + \sum_{k=0}^{n-1} {}_k\mathbf{X} \frac{\varkappa^k}{k!}, \tag{36} $$

where $\mathbf{\Phi}(\varkappa) = \left(\mathbf{I}_N \otimes (\mathbf{\Pi}^{\varrho}\, \mathbb{T}_d(\varkappa))^T\right)$ encapsulates the action of the fractional integral operational matrix on the basis.

6.3 Reformulation of the MFOCP

With the approximations (36) and (33), the cost functional (1) is transformed into a multivariate function of the unknown coefficients

$$J \approx \int_0^1 \mathbf{A}\left(\varkappa, {}^{d}\mathbf{X}(\varkappa), {}^{d}\mathbf{V}(\varkappa)\right) \mathrm{d}\varkappa = \mathcal{J}(\widehat{\mathbf{T}}, \widehat{\mathbf{U}}). \tag{37}$$

This integral can be efficiently evaluated using numerical quadrature, such as Gaussian integration. The inequality constraints (3) are handled by introducing a set of auxiliary slack variables $z_j(\varkappa)$, $j = 1, \ldots, s$, which transform the inequality constraints into equality constraints. This is achieved by adding the square of the slack variable to the original inequality constraint, ensuring non-negativity

$$\mathbf{C}_j\left(\varkappa, {}^{d}\mathbf{X}(\varkappa), {}^{d}\mathbf{V}(\varkappa)\right) + \left({}^{d}z_j(\varkappa)\right)^2 = 0. \tag{38}$$

The slack variables ${}^{d}z_j(\varkappa)$ are also approximated using fractional Taylor polynomials

$${}^{d}z_j(\varkappa) = \mathbf{Z}_j^T \mathbb{T}_d(\varkappa), \quad j = 1, \ldots, s. \tag{39}$$

This formulation ensures that the inequality constraints are satisfied by construction, as the squared term guarantees that the left-hand side is non-negative.

The inequality constraints (3) are handled by introducing a set of auxiliary slack variables $z_j(\varkappa)$, $j = 1, \ldots, s$, converting them into equality constraints

$$\mathbf{C}_j\left(\varkappa, {}^{d}\mathbf{X}(\varkappa), {}^{d}\mathbf{V}(\varkappa)\right) + \left({}^{d}z_j(\varkappa)\right)^2 = 0. \tag{40}$$

The slack variables are also approximated using fractional Taylor polynomials

$${}^{d}z_j(\varkappa) = \mathbf{Z}_j^T \mathbb{T}_d(\varkappa), \quad j = 1, \ldots, s. \tag{41}$$

Substituting the approximations Eqs. (36), (33), and Eq. (41) into the system dynamics Eq. (2) and the constraints (40) yields the residual equations

$$\mathbf{H}_0(\varkappa; \widehat{\mathbf{T}}, \widehat{\mathbf{U}}) = {}^{\mathrm{C}}\mathcal{D}_{\varkappa}^{\varrho}\, {}^{d}\mathbf{X}(\varkappa) - \mathbf{B}\left(\varkappa, {}^{d}\mathbf{X}(\varkappa), {}^{d}\mathbf{V}(\varkappa)\right) = \mathbf{0}, \tag{42}$$

$$\mathbf{H}_j(\varkappa; \widehat{\mathbf{T}}, \widehat{\mathbf{U}}, \mathbf{Z}_j) = \mathbf{C}_j\left(\varkappa, {}^{d}\mathbf{X}(\varkappa), {}^{d}\mathbf{V}(\varkappa)\right) + \left(\mathbf{Z}_j^T \mathbb{T}_d(\varkappa)\right)^2 = 0, \quad j = 1, \ldots, s. \tag{43}$$

6.4 Galerkin projection and optimization

The Galerkin method mandates that the residuals (42) and (43) be orthogonal to the basis functions $\{\mathcal{T}_i(\varkappa)\}_{i=0}^{d}$. This projection transforms the continuous residual equations into a finite system of algebraic equations

$$\begin{aligned} \mathbf{H}_{0,i} &:= \int_0^1 \mathbf{H}_0(\varkappa)\, \mathcal{T}_i(\varkappa) \mathrm{d}\varkappa = \mathbf{0}, \\ \mathbf{H}_{j,i} &:= \int_0^1 \mathbf{H}_j(\varkappa)\, \mathcal{T}_i(\varkappa) \mathrm{d}\varkappa = 0, \end{aligned} \qquad \text{for } i = 0, \ldots, d,\ j = 1, \ldots, s. \tag{44}$$

The original MFOCP is now reduced to the constrained optimization problem of minimizing $\mathcal{J}(\widehat{\mathbf{T}}, \widehat{\mathbf{U}})$ subject to the constraints (44). This is solved by formulating the Lagrangian

$$\mathcal{L}(\widehat{\mathbf{T}}, \widehat{\mathbf{U}}, \{\mathbf{Z}_j\}, \{\lambda_{j,i}\}) = \mathcal{J}(\widehat{\mathbf{T}}, \widehat{\mathbf{U}}) + \sum_{j=0}^{s} \sum_{i=0}^{d} \lambda_{j,i}\, \mathbf{H}_{j,i}, \tag{45}$$

where $\lambda_{j,i}$ are Lagrange multipliers. The first-order necessary optimality conditions are given by

$$\frac{\partial \mathcal{L}}{\partial \widehat{\mathbf{T}}} = \mathbf{0}, \quad \frac{\partial \mathcal{L}}{\partial \widehat{\mathbf{U}}} = \mathbf{0}, \quad \frac{\partial \mathcal{L}}{\partial \mathbf{Z}_j} = \mathbf{0}, \quad \frac{\partial \mathcal{L}}{\partial \lambda_{j,i}} = \mathbf{H}_{j,i} = 0. \tag{46}$$

The system of equations (46) is typically large and nonlinear. It is solved numerically using an iterative method such as Newton's scheme. The Newton iteration is initialized with an initial guess for the unknown coefficients $\widehat{\mathbf{T}}^{(0)}$, $\widehat{\mathbf{U}}^{(0)}$, $\{\mathbf{Z}_j^{(0)}\}$, and $\{\lambda_{j,i}^{(0)}\}$. A practical initialization strategy is to use the solution of the unconstrained problem or a linearized version as the initial guess. For the problems considered in this work, initializing all coefficients to zero proved to be effective.

At each iteration k, the Newton update is computed by solving the linear system

$$\mathbf{J}^{(k)}\, \Delta \mathbf{p}^{(k)} = -\mathbf{F}^{(k)},$$

where $\mathbf{J}^{(k)}$ is the Jacobian matrix of the system (46) evaluated at the current iterate $\mathbf{p}^{(k)} = \left(\widehat{\mathbf{T}}^{(k)}, \widehat{\mathbf{U}}^{(k)}, \{\mathbf{Z}_j^{(k)}\}, \{\lambda_{j,i}^{(k)}\}\right)$, $\mathbf{F}^{(k)}$ is the residual vector, and $\Delta \mathbf{p}^{(k)}$ is the step. The solution is then updated as $\mathbf{p}^{(k+1)} = \mathbf{p}^{(k)} + \alpha^{(k)} \Delta \mathbf{p}^{(k)}$, where $\alpha^{(k)} \in (0, 1]$ is a damping parameter chosen to ensure a decrease in the residual norm.

The process repeats itself until the end point is achieved. The first criterion for termination of the algorithm is the following

$$\|\mathbf{F}^{(k)}\| < \epsilon_{\text{abs}} \quad \text{or} \quad \frac{\|\mathbf{F}^{(k)}\|}{\|\mathbf{F}^{(0)}\|} < \epsilon_{\text{rel}},$$

here, ϵ_{abs} and ϵ_{rel} are absolute and relative tolerances, respectively (e.g., 10^{-12} and 10^{-10}). Additionally, a limit on the maximum number of iterations (e.g., 100) is imposed to prevent excessive computation in case of slow convergence.

The solution yields the optimal coefficients $\widehat{\mathbf{T}}^{\star}$ and $\widehat{\mathbf{U}}^{\star}$, from which the approximate optimal state and control trajectories, ${}^{d}\mathbf{X}^{\star}(\varkappa)$ and ${}^{d}\mathbf{V}^{\star}(\varkappa)$, are reconstructed via Eqs. (36) and (33), respectively.

This marks the end of the development of the GFT approach for dealing with the constrained multi-dimensional MFOCPs. The fundamental part of the procedure, presented in algorithm 1, lies in the approximation of the fractional derivatives of the state and the control function by means of the fractional Taylor polynomials, determination of the state with the help of the operational matrix found, and satisfaction of the system dynamics as well as other constraints due to Galerkin projection. The obtained NLP is solved with the use of Newton's method. The result of the method is the optimal set of coefficients $\widehat{\mathbf{T}}^{*}$ and $\widehat{\mathbf{U}}^{*}$, from which the optimal state trajectory, ${}^{d}\mathbf{X}^{*}(\varkappa)$, and the optimal control trajectory, ${}^{d}\mathbf{V}^{*}(\varkappa)$, are computed using formulas Eqs. (36) and (33), respectively. The performance of the suggested technique will be demonstrated and discussed in the next section.

Algorithm 1 The GFT method for constrained MFOCPs

Input: ϱ, d, $\mathbf{A}$, $\mathbf{B}$, $\mathbf{C}_i$, ${}_i\mathbf{X}$, s, dimension N
Output: Optimal state ${}^d\mathbf{X}^*(\varkappa)$ and control ${}^d\mathbf{V}^*(\varkappa)$
Set maximum iterations $N_{\max}$, tolerance ϵ
Initialize coefficient matrices $\widehat{\mathbf{T}}^{(0)}$, $\widehat{\mathbf{U}}^{(0)}$, $\mathbf{Z}_j^{(0)}$ for $j = 1, \ldots, s$
Approximate fractional derivative: ${}^{\mathrm{C}}\mathcal{D}_{\varkappa}^{\varrho}{}^d\mathbf{X}(\varkappa) = (\mathbf{I}_N \otimes \mathbb{T}_d(\varkappa)^T)\widehat{\mathbf{T}}^T$
Approximate control: ${}^d\mathbf{V}(\varkappa) = (\mathbf{I}_N \otimes \mathbb{T}_d(\varkappa)^T)\widehat{\mathbf{U}}^T$
Recover state: ${}^d\mathbf{X}(\varkappa) = \mathbf{\Phi}(\varkappa)\widehat{\mathbf{T}}^T + \sum_{\kappa=0}^{m-1} {}_\kappa\mathbf{X}\frac{\varkappa^\kappa}{\kappa!}$
for $j = 1$ to s **do**
    Approximate slack variables: ${}^d z_j(\varkappa) = \mathbf{Z}_j^T\mathbb{T}_d(\varkappa)$
    Convert inequalities: $\mathbf{C}_j(\varkappa, {}^d\mathbf{X}(\varkappa), {}^d\mathbf{V}(\varkappa)) + ({}^d z_j(\varkappa))^2 = 0$
end for
Compute dynamics residual: $\mathbf{H}_0(\varkappa) = {}^{\mathrm{C}}\mathcal{D}_{\varkappa}^{\varrho}{}^d\mathbf{X}(\varkappa) - \mathbf{B}(\varkappa, {}^d\mathbf{X}(\varkappa), {}^d\mathbf{V}(\varkappa))$
for $j = 1$ to s **do**
    Compute constraint residual: $\mathbf{H}_j(\varkappa) = \mathbf{C}_j(\varkappa, {}^d\mathbf{X}(\varkappa), {}^d\mathbf{V}(\varkappa)) + (\mathbf{Z}_j^T\mathbb{T}_d(\varkappa))^2$
end for
for $i = 0$ to d **do**
    Project dynamics: $\mathbf{H}_{0,i} = \int_0^1 \mathbf{H}_0(\varkappa)\mathcal{T}_i(\varkappa)d\varkappa = 0$
    for $j = 1$ to s **do**
        Project constraints: $\mathbf{H}_{j,i} = \int_0^1 \mathbf{H}_j(\varkappa)\mathcal{T}_i(\varkappa)d\varkappa = 0$
    end for
end for
Formulate cost: $\mathcal{J}(\widehat{\mathbf{T}}, \widehat{\mathbf{U}}) = \int_0^1 \mathbf{A}(\varkappa, {}^d\mathbf{X}(\varkappa), {}^d\mathbf{V}(\varkappa))d\varkappa$
Construct Lagrangian: $\mathcal{L} = \mathcal{J} + \sum_{j=0}^{s}\sum_{i=0}^{d} \lambda_{j,i}\mathbf{H}_{j,i}$
Solve optimality conditions using Newton's method:
    $\frac{\partial\mathcal{L}}{\partial\widehat{\mathbf{T}}} = 0$, $\frac{\partial\mathcal{L}}{\partial\widehat{\mathbf{U}}} = 0$
for $j = 1$ to s **do**
        $\frac{\partial\mathcal{L}}{\partial\mathbf{Z}_j} = 0$
end for
for $j = 0$ to s **do**
    for $i = 0$ to d **do**
            $\mathbf{H}_{j,i} = 0$
    end for
end for
while $k < N_{\max}$ and $\|\nabla\mathcal{L}\| > \epsilon$ **do**
    Update coefficients using Newton iteration: $\widehat{\mathbf{T}}^{(k+1)}, \widehat{\mathbf{U}}^{(k+1)}, \mathbf{Z}_j^{(k+1)}$
    $k \leftarrow k + 1$
    Recompute Lagrangian $\mathcal{L}$ and its gradient $\nabla\mathcal{L}$
end while
Reconstruct optimal state: ${}^d\mathbf{X}^*(\varkappa) = \mathbf{\Phi}(\varkappa)(\widehat{\mathbf{T}}^*)^T + \sum_{\kappa=0}^{m-1} {}_\kappa\mathbf{X}\frac{\varkappa^\kappa}{\kappa!}$
Reconstruct optimal control: ${}^d\mathbf{V}^*(\varkappa) = (\mathbf{I}_N \otimes \mathbb{T}_d(\varkappa)^T)(\widehat{\mathbf{U}}^*)^T$

7 Numerical examples

This section demonstrates the efficacy, accuracy, and convergence properties of the proposed GFT method by applying it to four benchmark MFOCPs. The results are compared with existing methods from the literature.

Example 1

We first consider a classic linear time-invariant MFOCP [9, 34]:

$$\begin{cases} \min J = \dfrac{1}{2}\displaystyle\int_0^1 \left(\mathbf{X}^2(\varkappa) + \mathbf{V}^2(\varkappa)\right) \mathrm{d}\varkappa, \\ {}^{\mathrm{C}}\mathcal{D}_{\varkappa}^{\varrho}\mathbf{X}(\varkappa) = -\mathbf{X}(\varkappa) + \mathbf{V}(\varkappa), \\ \mathbf{X}(0) = 1. \end{cases} \tag{47}$$

For the integer-order case ($\varrho = 1$), the exact solution is known

$$\begin{aligned} \mathbf{X}(\varkappa) &= \cosh(\sqrt{2}\varkappa) + \beta \sinh(\sqrt{2}\varkappa), \\ \mathbf{V}(\varkappa) &= (1 + \sqrt{2}\alpha)\cosh(\sqrt{2}\varkappa) + (\sqrt{2} + \alpha)\sinh(\sqrt{2}\varkappa), \end{aligned}$$

where $\alpha = -\frac{\cosh(\sqrt{2}) + \sqrt{2}\sinh(\sqrt{2})}{\sqrt{2}\cosh(\sqrt{2}) + \sinh(\sqrt{2})}$.

For $d = 4$ and $\varrho = 1$, the approximate solution is ${}^{\mathrm{C}}\mathcal{D}_{\varkappa}^{1}({}^{4}\mathbf{X}(\varkappa)) = \mathbf{T}\mathbb{T}_4(\varkappa)$, and ${}^{4}\mathbf{V}(\varkappa) = \mathbf{U}\mathbb{T}_4(\varkappa)$, where

$$\mathbb{T}_4(\varkappa) = \begin{bmatrix} 1 \\ \varkappa \\ \varkappa^2 \\ \varkappa^3 \\ \varkappa^4 \end{bmatrix},$$

$${}^{\mathrm{R.L}}\mathcal{I}^{1}\mathbb{T}_4(\varkappa) = \begin{bmatrix} \varkappa \\ 1/2\,\varkappa^2 \\ 1/3\,\varkappa^3 \\ 1/4\,\varkappa^4 \\ 1/5\,\varkappa^5 \end{bmatrix}.$$

Implementing GFT method, we obtain

$$\begin{aligned} {}^{4}\mathbf{X}(\varkappa) = &-1.385676059\,\varkappa + 0.9977935270\,\varkappa^2 - 0.4511874397\,\varkappa^3 + 0.1436498327\,\varkappa^4 \\ &- 0.02261032760\,\varkappa^5 + 1, \end{aligned}$$

$${}^{4}\mathbf{V}(\varkappa) = -0.3857658777 + 0.6126044078\,\varkappa - 0.3746178050\,\varkappa^2 + 0.1736674070\,\varkappa^3 - 0.0259325535\,\varkappa^4.$$

For $d' = 6$, from the Theorem 3 by solving the error problem

$$\begin{cases} \min\ J_4 = \frac{1}{2}\displaystyle\int_0^1 \left({}^{4}\mathbb{E}^{\mathbf{X}}(\varkappa) + {}^{4}\,\mathbf{X}(\varkappa)\right)^2 + \left({}^{4}\mathbb{E}^{\mathbf{V}}(\varkappa) + {}^{4}\,\mathbf{V}(\varkappa)\right)^2 \mathrm{d}\varkappa, \\ \text{subject to} \\ \quad {}^{\mathrm{C}}\mathcal{D}_{\varkappa}^{1}\left({}^{4}\mathbb{E}^{\mathbf{X}}(\varkappa) + {}^{4}\mathbf{X}(\varkappa)\right) = -\left({}^{4}\mathbb{E}^{\mathbf{X}}(\varkappa) + {}^{4}\mathbf{X}(\varkappa)\right) + \left({}^{4}\mathbb{E}^{\mathbf{V}}(\varkappa) + {}^{4}\mathbf{V}(\varkappa)\right), \\ \quad {}^{4}\mathbb{E}^{\mathbf{X}}(0) = 1 - {}^{4}\mathbf{X}(0), \end{cases} \tag{48}$$

by the GFT method, we get the approximation for the error:

$$
\begin{aligned}
{}^{6,4}\mathbb{E}^{\mathbf{V}}(\varkappa) = &-0.00005137490 + 0.00152897557\,\varkappa - 0.01075792085\,\varkappa^2 \\
&+ 0.02927585581\,\varkappa^3 - 0.0346006431\,\varkappa^4 + 0.01601343516\,\varkappa^5 - 0.00136416711\,\varkappa^6,
\end{aligned}
$$

$$
\begin{aligned}
{}^{6,4}\mathbb{E}^{\mathbf{X}}(\varkappa) = &-0.00014294693\,\varkappa + 0.002212689080\,\varkappa^2 - 0.01076435777\,\varkappa^3 \\
&+ 0.02290220032\,\varkappa^4 - 0.02299284888\,\varkappa^5 + 0.009998361823\,\varkappa^6 - 0.001213096546\,\varkappa^7.
\end{aligned}
$$

Figure 1 displays the absolute error in the state $\mathbf{X}(\varkappa)$ and the corresponding results for the control $\mathbf{V}(\varkappa)$ for the initial approximation ($d = 4$). These figures confirm that the proposed error estimation technique provides a reliable measure of the approximation error, even without knowledge of the exact solution.

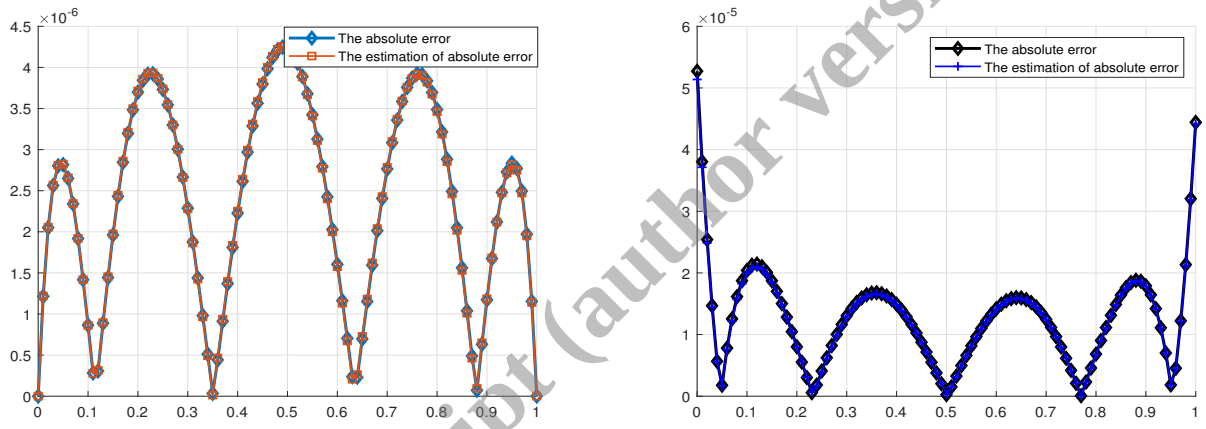

(a) Error of $\mathbf{X}$ (b) Error of $\mathbf{V}$

Figure 1: Error analysis for the state variable in Example 1 ($\varrho = 1$) using degree $d = 4$ and error estimation degree $d' = 6$ obtained from Theorem 3, (a) for $\mathbf{X}$ and (b) for $\mathbf{V}$.

Figure 2 illustrates the state solution $\mathbf{X}(\varkappa)$ and the control $\mathbf{V}(\varkappa)$ for $\varrho = 1$. The high accuracy achieved with $d = 4$.

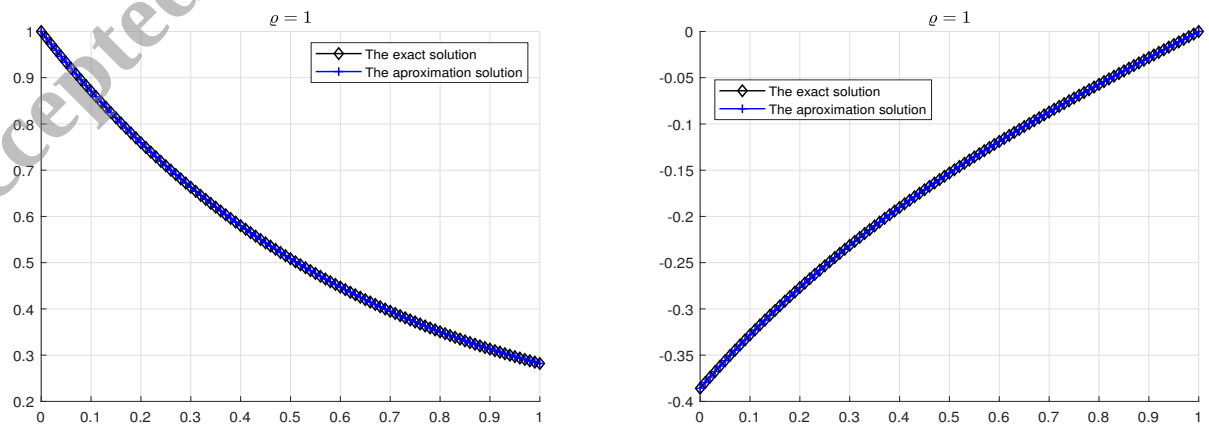

(a) Solutions of $\mathbf{X}$ (b) Solution of $\mathbf{U}$

Figure 2: Exact and approximate solutions of $\mathbf{X}(\varkappa)$ for (a) and $\mathbf{V}(\varkappa)$ for (b) with $d = 4$ and $\varrho = 1$ in Example 1.

Figure 3 shows the $\mathbf{X}(\varkappa)$ for (a) and $\mathbf{V}(\varkappa)$ for (b) with $\varrho = 0.7, 0.8$ and 1.

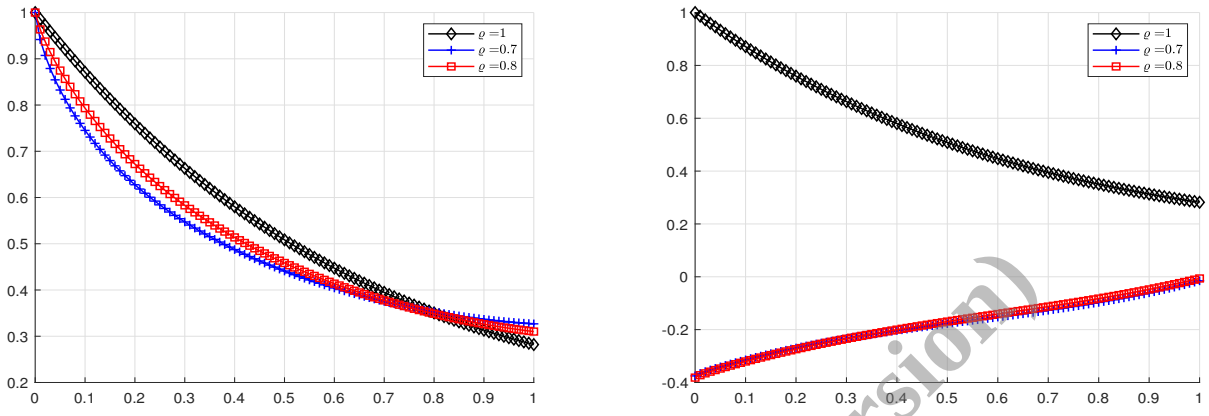

(a) Approximate solutions $\mathbf{X}$ (b) Approximate solutions $\mathbf{V}$

Figure 3: Approximate solution of $\mathbf{X}(\varkappa)$ for (a) and $\mathbf{V}(\varkappa)$ for (b) with $d = 4$ and $\varrho = 1$, $\varrho = 0.7$, 0.8, 1 in Example 1.

Table 1 presents a quantitative comparison of the absolute error in $\mathbf{X}(\varkappa)$ for $d = 4$ against the methods reported in [9] and [34]. The results obtained by the proposed method, both before and after error correction, exhibit superior or highly competitive accuracy across the entire domain, with a CPU time of 0.313 seconds.

Table 1: $X(\varkappa)$ when $\varrho = 1$, $d = 4$, and $d' = 6$.

	Method [9]	Method [34]	Present method (Degree $d = 4$)	
$\varkappa$			The absolute error	The estimation of absolute error
0	0	8.99×10^{-5}	0	0
0.1	1.56×10^{-5}	4.77×10^{-5}	8.64×10^{-7}	8.63×10^{-7}
0.2	2.64×10^{-5}	3.25×10^{-5}	3.69×10^{-6}	3.70×10^{-6}
0.3	3.61×10^{-5}	7.74×10^{-5}	2.28×10^{-6}	2.28×10^{-6}
0.4	3.89×10^{-6}	2.13×10^{-5}	2.22×10^{-6}	2.24×10^{-6}
0.5	3.81×10^{-5}	6.43×10^{-5}	4.23×10^{-6}	4.23×10^{-6}
0.6	4.94×10^{-5}	1.03×10^{-4}	1.60×10^{-6}	1.58×10^{-6}
0.7	1.01×10^{-5}	1.12×10^{-4}	1.58×10^{-6}	1.58×10^{-6}
0.8	5.51×10^{-5}	9.14×10^{-5}	3.48×10^{-6}	3.46×10^{-6}
0.9	5.53×10^{-5}	9.41×10^{-5}	1.17×10^{-6}	1.18×10^{-6}

As an example, let us show how to apply the framework of error estimation to Example 1. We begin with an initial guess of $d = 4$ and then use the error estimation technique to solve the problem of optimal error control (48) with $d' = 6$. The corrected results are obtained through

$$^{6}\mathbf{X}_{\text{corrected}}(\varkappa) = {}^{4}\mathbf{X}(\varkappa) + {}^{6,4}\mathbb{E}^{\mathbf{X}}(\varkappa),$$
$$^{6}\mathbf{V}_{\text{corrected}}(\varkappa) = {}^{4}\mathbf{V}(\varkappa) + {}^{6,4}\mathbb{E}^{\mathbf{V}}(\varkappa).$$

From Table 2, it can be seen that there has been a significant enhancement in terms of numerical results as a result of error correction. In particular, the maximum absolute error of the state variables is lowered from $\mathcal{O}(10^{-6})$ to $\mathcal{O}(10^{-8})$, demonstrating the effectiveness of the proposed error estimation and correction framework. The following numerical illustration

Table 2: Error correction performance for Example 1 ($\varrho = 1$)

$\varkappa$	$\lvert X_{\text{exact}} - {}^{4}\mathbf{X}\rvert$	$\lvert X_{\text{exact}} - {}^{6}\mathbf{X}_{\text{corrected}}\rvert$
0.2	3.69×10^{-6}	2.15×10^{-8}
0.5	4.23×10^{-6}	3.08×10^{-8}
0.8	3.48×10^{-6}	1.92×10^{-8}

verifies that the error estimation process offers not just a dependable means to quantify the approximation error, but also offers scope for reducing the error using an iterative technique.

In order to test the stability of our model expressed in (47), we made an infinitesimal disturbance to the initial value. This was achieved by slightly altering the initial condition to $\mathbf{X}(0) = 1.00001$, thus forming a disturbed problem. In order to determine the size of the disturbance, we measured the error value $|X_{\text{exact}} - \mathbf{X}^{(4)}|$ (Err) for the unperturbed problem. Furthermore, the absolute error for the disturbed problem (Err.per) was calculated by comparing the exact solution to its approximate version $\mathbf{X}_p^{(4)}$. From Table 3 and Table 4, it is evident that the results of the disturbed problem agree with the exact solution, thus proving the stability of the model.

Table 3: The $\mathbf{X}$, $\mathbf{X}_4$, $\mathbf{X}_4^p$, absolute error and perturbed absolute error for different values with $d = 4$ for Example 1.

$\varkappa$	$\mathbf{X}$	$\mathbf{X}_4$	$\mathbf{X}_4^p$	Err	Err.per
0.0	1.0000000000	1.0000000000	1.0000100000	0.00×10^{0}	1.00×10^{-5}
0.1	0.8709724165	0.8709732758	0.8709819855	8.59×10^{-7}	9.57×10^{-6}
0.2	0.7593933330	0.7593896350	0.7593972289	3.70×10^{-6}	3.90×10^{-6}
0.3	0.6630274463	0.6630251654	0.6630317956	2.28×10^{-6}	4.35×10^{-6}
0.4	0.5799442241	0.5799464566	0.5799522560	2.23×10^{-6}	8.03×10^{-6}
0.5	0.5084792307	0.5084834659	0.5084885508	4.24×10^{-6}	9.32×10^{-6}
0.6	0.4472007826	0.4472023835	0.4472068555	1.60×10^{-6}	6.07×10^{-6}
0.7	0.3948812668	0.3948784972	0.3948824460	2.77×10^{-6}	1.18×10^{-6}
0.8	0.3504725478	0.3504690582	0.3504725629	3.49×10^{-6}	1.51×10^{-8}
0.9	0.3130849700	0.3130861460	0.3130892768	1.18×10^{-6}	4.31×10^{-6}
1.0	0.2819695346	0.2819695337	0.2819723534	9.08×10^{-10}	2.82×10^{-6}

Table 4: The $\mathbf{V}$, $\mathbf{V}_4$, $\mathbf{V}_4^p$, absolute error and perturbed absolute error for different values with $d = 4$ for Example 1.

$\varkappa$	$\mathbf{V}$	$\mathbf{V}_4$	$\mathbf{V}_4^p$	Err	Err.per
0.0	-0.3858185962	-0.3857659576	-0.3857698152	5.26×10^{-5}	4.88×10^{-5}
0.1	-0.3280601444	-0.3280805262	-0.3280838070	2.04×10^{-5}	2.37×10^{-5}
0.2	-0.2768738381	-0.2768818298	-0.2768845986	7.99×10^{-6}	1.08×10^{-5}
0.3	-0.2312342439	-0.2312211794	-0.2312234916	1.31×10^{-5}	1.08×10^{-5}
0.4	-0.1902270475	-0.1902121357	-0.1902140379	1.49×10^{-5}	1.30×10^{-5}
0.5	-0.1530307372	-0.1530305092	-0.1530320395	2.28×10^{-7}	1.30×10^{-6}
0.6	-0.1189001461	-0.1189143601	-0.1189155493	1.42×10^{-5}	1.54×10^{-5}
0.7	-0.0871515239	-0.0871639983	-0.0871648699	1.25×10^{-5}	1.33×10^{-5}
0.8	-0.0571488391	-0.0571419835	-0.0571425549	6.86×10^{-6}	6.28×10^{-6}
0.9	-0.0282910373	-0.0282731251	-0.0282734078	1.79×10^{-5}	1.76×10^{-5}
1.0	-0.0000000000	-0.0000444822	-0.0000444827	4.45×10^{-5}	4.45×10^{-5}

Example 2

Next, we solve an MFOCP featuring both state and control inequality constraints [33]:

$$\begin{cases} \min J = \displaystyle\int_0^1 \Big(\mathbf{X}^2 + \mathbf{V}^2 + 2\varkappa^{3/2}\mathbf{X} - 2(1-\varkappa^{3/2})\mathbf{V}\Big)\,\mathrm{d}\varkappa, \\ \text{subject to: } {}^{\mathrm{C}}\mathcal{D}_{\varkappa}^{3/2}\mathbf{X}(\varkappa) = \dfrac{3\sqrt{\pi}}{4}(\mathbf{X}(\varkappa) - \mathbf{V}(\varkappa)), \\ \quad \mathbf{X}(\varkappa) \le 0, \quad 0 \le V(\varkappa) \le 1, \\ \quad \mathbf{X}(0) = \mathbf{X}'(0) = 0. \end{cases} \tag{49}$$

The exact solution is $\mathbf{X}(\varkappa) = -\varkappa^{3/2}$, $\mathbf{V}(\varkappa) = 1 - \varkappa^{3/2}$, yielding an optimal cost $J = -0.7$.

For $d = 1$ and $\varrho = \frac{2}{3}$, the approximate solution is ${}^{\mathrm{C}}\mathcal{D}_{\varkappa}^{\frac{2}{3}}({}^{1}\mathbf{X}(\varkappa)) = \mathbf{T}\mathbb{T}_1(\varkappa)$ and ${}^{1}\mathbf{V}(\varkappa) = \mathbf{U}\mathbb{T}_1(\varkappa)$, where

$$\mathbb{T}_1(\varkappa) = \begin{bmatrix} 1 \\ \varkappa^{3/2} \end{bmatrix},$$

$${}^{\mathrm{R.L}}\mathcal{I}_{\frac{2}{3}}\mathbb{T}_1(\varkappa) = \begin{bmatrix} 4/3\,\frac{\varkappa^{3/2}}{\sqrt{\pi}} \\ 1/8\,\varkappa^{3}\sqrt{\pi} \end{bmatrix}.$$

Using GFT approach, it follows that

$${}^{1}\mathbf{X}(\varkappa) = -1.772453851\,\frac{\varkappa^{3/2}}{\sqrt{\pi}} - 0.0000000001127579925\,\varkappa^{3}\sqrt{\pi},$$
$${}^{1}\mathbf{V}(\varkappa) = 0.9999999999 - 0.9999999995\,\varkappa^{3/2}.$$

For $d = 4$, the approximate solution is ${}^{4}\mathbf{X}(\varkappa) = \mathbf{T}\mathbb{T}_4(\varkappa)$, where

$$\mathbb{T}_4(\varkappa) = \begin{bmatrix} 1 \\ \varkappa^{3/2} \\ \varkappa^{3} \\ \varkappa^{9/2} \\ \varkappa^{6} \end{bmatrix},$$

$${}^{\mathrm{R.L}}\mathcal{I}_{\frac{2}{3}}\mathbb{T}_4(\varkappa) = \begin{bmatrix} 4/3\,\frac{\varkappa^{3/2}}{\sqrt{\pi}} \\ 1/8\,\varkappa^{3}\sqrt{\pi} \\ \frac{64\,\varkappa^{9/2}}{315\,\sqrt{\pi}} \\ \frac{21\,\varkappa^{6}\sqrt{\pi}}{512} \\ \frac{4096\,\varkappa^{15/2}}{45045\,\sqrt{\pi}} \end{bmatrix}.$$

Apply the GFT method in Section 6, we obtain

$$
\begin{aligned}
{}^{4}\mathbf{X}(\varkappa) = &- 1.772453850905053\,\frac{\varkappa^{3/2}}{\sqrt{\pi}} - 1.099993449325995 \times 10^{-12}\,\varkappa^{3}\sqrt{\pi} \\
&+ 8.659083640613335 \times 10^{-12}\,\frac{\varkappa^{9/2}}{\sqrt{\pi}} - 2.816324877899974 \times 10^{-12}\,\varkappa^{6}\sqrt{\pi} \\
&+ 3.186419499822500 \times 10^{-12}\,\frac{\varkappa^{15/2}}{\sqrt{\pi}},
\end{aligned}
$$

$$
\begin{aligned}
{}^{4}\mathbf{V}(\varkappa) = &0.9999999999999374 - 0.9999999999984059\,\varkappa^{3/2} - 7.537931752503131 \times 10^{-12}\,\varkappa^{3} \\
&+ 1.192939665528195 \times 10^{-11}\,\varkappa^{9/2} - 6.007609032379279 \times 10^{-12}\,\varkappa^{6}.
\end{aligned}
$$

Figures 4 and subsequent figures show excellent agreement between the numerical and exact solutions even for low approximation degrees ($d = 1$ and 4). The computed cost functional J (Table 5) achieves machine-level precision ($-0.700000\ldots$), outperforming the reference method. Tables 6 and 7 confirm the high accuracy of the state and control approximations.

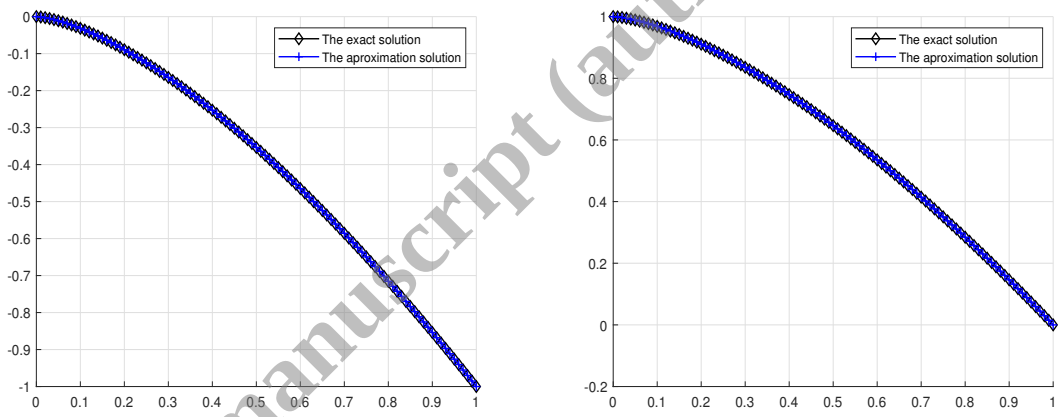

(a) State $\mathbf{X}(\varkappa)$ (b) Control $\mathbf{V}(\varkappa)$

Figure 4: Numerical vs. exact solutions for $d = 1$.

Table 5: Comparison of the cost functional J for Example 2.

Degree (d)	Method in [33]	Present Method	CPU times (s)
1	-0.700001315194399	-0.7000000000000000	0.110
4	-0.700000007265492	-0.7000000000000000	0.406

Table 6: Absolute error of $\mathbf{X}(\varkappa)$ of $\varkappa$ in Example 2 with degree $d = 4$.

$\varkappa$	Method [33]	Present method
0	0	0
0.1	6.8×10^{-11}	6.4×10^{-15}
0.2	6.8×10^{-11}	1.0×10^{-14}
0.3	6.8×10^{-11}	8.5×10^{-15}
0.4	1.9×10^{-9}	1.8×10^{-15}
0.5	1.9×10^{-9}	3.5×10^{-15}
0.6	5.1×10^{-9}	3.1×10^{-15}
0.7	7.2×10^{-9}	2.3×10^{-15}
0.8	7.2×10^{-9}	7.3×10^{-15}
0.9	7.2×10^{-9}	5.8×10^{-15}
1	1.4×10^{-8}	2.5×10^{-15}

Table 7: Absolute error of $\mathbf{V}(\varkappa)$ of $\varkappa$ in Example 2 with degree $d = 4$.

$\varkappa$	Method [33]	Present method
0	3.5×10^{-10}	6.2×10^{-14}
0.1	4.8×10^{-9}	1.9×10^{-14}
0.2	9.0×10^{-9}	2.7×10^{-14}
0.3	1.3×10^{-8}	4.4×10^{-14}
0.4	1.7×10^{-8}	2.6×10^{-14}
0.5	2.1×10^{-8}	7.9×10^{-15}
0.6	1.6×10^{-8}	3.2×10^{-14}
0.7	1.1×10^{-8}	2.4×10^{-14}
0.8	5.6×10^{-9}	1.4×10^{-14}
0.9	2.4×10^{-10}	3.5×10^{-14}
1	5.1×10^{-9}	8.4×10^{-14}

Figures 5-6 The absolute errors in the state and control with $d = 4$ and $d = 1$.

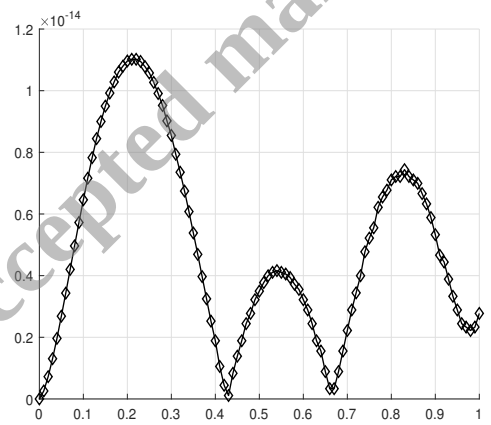

(a) State $\mathbf{X}(\varkappa)$

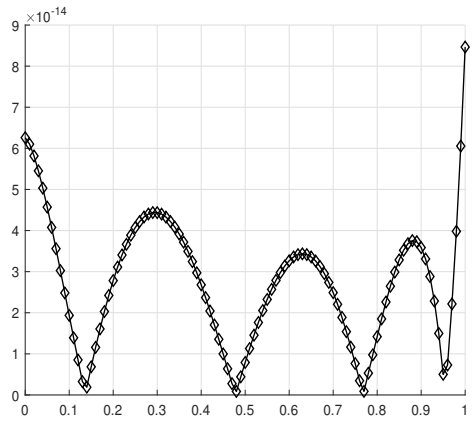

(b) Control $\mathbf{V}(\varkappa)$

Figure 5: Absolute error for the state function $\mathbf{X}(\vartheta)$ for (a) and the control function $\mathbf{V}(\vartheta)$ for (b) with $d = 4$ for Example 2.

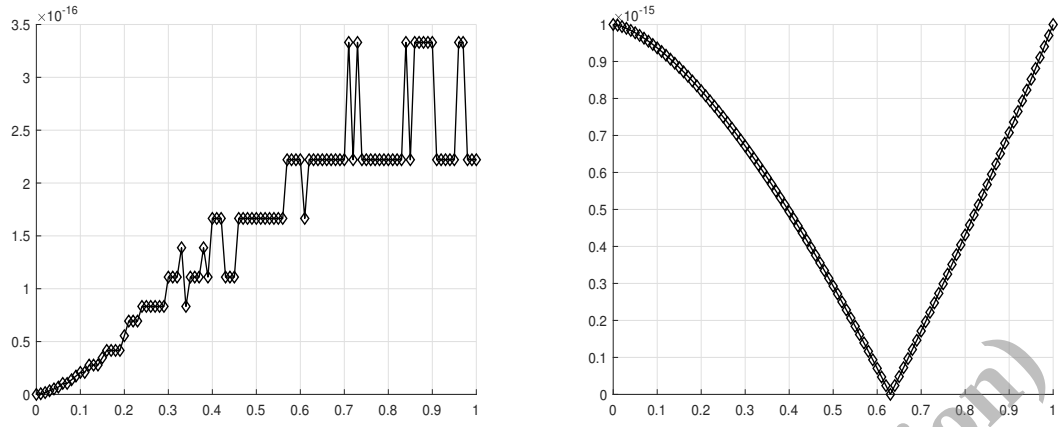

(a) State $\mathbf{X}(\varkappa)$ (b) Control $\mathbf{V}(\varkappa)$

Figure 6: Absolute error for the state function $\mathbf{X}(\vartheta)$ for (a) and the control function $\mathbf{V}(\vartheta)$ for (b) with $d = 1$ for Example 2.

Example 3

Finally, we consider an MFOCP designed to have a known exact solution [33]:

$$\begin{cases} \min J = \displaystyle\int_0^1 \left[(\mathbf{X}(\varkappa) - \varkappa^{\varrho})^2 + (\mathbf{V}(\varkappa) - \varkappa^{\varrho} - \Gamma(\varrho+1))^2\right] \mathrm{d}\varkappa, \\ \text{subject to: } {}^{\mathrm{C}}\mathcal{D}_{\varkappa}^{\varrho}\mathbf{X}(\varkappa) = -\mathbf{X}(\varkappa) + \mathbf{V}(\varkappa), \\ \quad \mathbf{X}(0) = 0. \end{cases} \tag{50}$$

The exact solution is $\mathbf{X}(\varkappa) = \varkappa^{\varrho}$, $\mathbf{V}(\varkappa) = \varkappa^{\varrho} + \Gamma(\varrho+1)$. For $d = 1$, the approximate solution is ${}^{\mathrm{C}}\mathcal{D}_{\varkappa}^{\varrho}({}^{1}\mathbf{X}(\varkappa)) = \mathbf{T}\,\mathbb{T}_1(\varkappa)$ and ${}^{1}\mathbf{V}(\varkappa) = \mathbf{U}\,\mathbb{T}_1(\varkappa)$, where $\mathbf{T} = [\mathbf{T}_0, \mathbf{T}_1]$, $\mathbf{U} = [u_0, u_1]$, and

$$\mathbb{T}_1(\varkappa) = \begin{bmatrix} 1 \\ \varkappa^{\varrho} \end{bmatrix}, \qquad {}^{\mathrm{R.L}}\mathcal{I}^{\varrho}\mathbb{T}_1(\varkappa) = \begin{bmatrix} \frac{\varkappa^{\varrho}}{\Gamma(\varrho+1)} \\ \frac{\varkappa^{2\,\varrho}\Gamma(\varrho+1)}{\Gamma(2\,\varrho+1)} \end{bmatrix}.$$

Using GFT approach, and solving (46), it follows that

$$\mathbf{T}_0 = \Gamma(\varrho+1), \quad \mathbf{T}_1 = 0, \quad u_0 = \Gamma(\varrho+1), \quad u_1 = 1,$$

then

$$\begin{cases} {}^{1}\mathbf{X}(\varkappa) = \varkappa^{\varrho}, \\ {}^{1}\mathbf{V}(\varkappa) = \Gamma(\varrho+1) + \varkappa^{\varrho}. \end{cases} \tag{51}$$

For $d' = 2$, from Theorem 3

$$\begin{cases} \min\ J = \displaystyle\int_0^1 \left[\left({}^{1}\mathbb{E}^{\mathbf{X}}(\varkappa) + {}^{1}\mathbf{X}(\varkappa) - \varkappa^{\varrho}\right)^2 + \left({}^{1}\mathbb{E}^{\mathbf{V}}(\varkappa) + {}^{1}\,\mathbf{V}(\varkappa) - \varkappa^{\varrho} - \Gamma(\varrho+1)\right)^2\right] \mathrm{d}\varkappa, \\ \text{subject to } 0 < \varrho \le 1, \\ \quad {}^{\mathrm{C}}\mathcal{D}_{\varkappa}^{\varrho}\left({}^{1}\mathbb{E}^{\mathbf{X}}(\varkappa) + {}^{1}\mathbf{X}(\varkappa)\right) = -\left({}^{1}\mathbb{E}^{\mathbf{X}}(\varkappa) + {}^{1}\mathbf{X}(\varkappa)\right) + \left({}^{1}\mathbb{E}^{\mathbf{V}}(\varkappa) + {}^{1}\mathbf{V}(\varkappa)\right), \\ \quad {}^{1}\mathbb{E}^{\mathbf{X}}(0) = -{}^{1}\mathbf{X}(0), \end{cases} \tag{52}$$

so

$$\begin{cases} \min\ J=\displaystyle\int_0^1 \left[\left({}^{1}\mathbb{E}^{\mathbf{X}}(\varkappa)\right)^2+\left({}^{1}\mathbb{E}^{\mathbf{V}}(\varkappa)\right)^2\right]\mathrm{d}\varkappa, \\ \text{subject to } 0<\varrho\leq 1, \\ \qquad {}^{\mathrm{C}}\mathcal{D}^{\varrho}_{\varkappa}\,{}^{1}\mathbb{E}^{\mathbf{X}}(\varkappa)=-{}^{1}\mathbb{E}^{\mathbf{X}}(\varkappa)+{}^{1}\mathbb{E}^{\mathbf{V}}(\varkappa),\quad {}^{1}\mathbb{E}^{\mathbf{X}}(0)=0, \end{cases} \tag{53}$$

so the approximate solution is ${}^{\mathrm{C}}\mathcal{D}^{\varrho}_{\varkappa}({}^{2,1}\mathbb{E}^{\mathbf{X}}(\varkappa))=\mathbf{T}^{\mathbb{E}^{\mathbf{X}}}\mathbb{T}_2(\varkappa)$, and ${}^{2,1}\mathbb{E}^{\mathbb{V}}(\varkappa)=\mathbf{U}^{\mathbb{E}^{\mathbf{V}}}\mathbb{T}_2(\varkappa)$, where

$$\mathbf{T}^{\mathbb{E}^{\mathbf{X}}}=\left[\mathbf{T}_0^{\mathbb{E}^{\mathbf{X}}},\mathbf{T}_1^{\mathbb{E}^{\mathbf{X}}},\mathbf{T}_2^{\mathbb{E}^{\mathbf{X}}}\right],\qquad \mathbf{U}^{\mathbb{E}^{\mathbf{V}}}=\left[u_0^{\mathbb{E}^{\mathbf{V}}},u_1^{\mathbb{E}^{\mathbf{V}}},u_2^{\mathbb{E}^{\mathbf{V}}}\right],$$

and

$$\mathbb{T}_2(\varkappa)=\begin{bmatrix}1\\ \varkappa^{\varrho}\\ (\varkappa^{\varrho})^2\end{bmatrix},$$

$${}^{\mathrm{R.L}}\mathcal{I}^{\varrho}\mathbb{T}_2(\varkappa)=\begin{bmatrix}\frac{\varkappa^{\alpha}}{\Gamma(\varrho+1)}\\ \frac{\varkappa^{2\,\varrho}\Gamma(\varrho+1)}{\Gamma(2\,\varrho+1)}\\ \frac{\varkappa^{3\,\varrho}\Gamma(2\,\varrho+1)}{\Gamma(3\,\varrho+1)}\end{bmatrix}.$$

Employing GFT procedure, solving (46), it follows that

$$\mathbf{T}_0^{\mathbb{E}^{\mathbf{X}}}=\mathbf{T}_1^{\mathbb{E}^{\mathbf{X}}}=\mathbf{T}_2^{\mathbb{E}^{\mathbf{X}}}=u_0^{\mathbb{E}^{\mathbf{V}}}=u_1^{\mathbb{E}^{\mathbf{V}}}=u_2^{\mathbb{E}^{\mathbf{V}}}=0,$$

then, we get the approximation for the error ${}^{2,1}\mathbb{E}^{\mathbf{V}}(\varkappa)={}^{2,1}\mathbb{E}^{\mathbf{X}}(\varkappa)=0$ Thus, Eq. (51) represents the exact solution to Problem (50).

For $d=2$, the approximate solution is ${}^{\mathrm{C}}\mathcal{D}^{\varrho}_{\varkappa}({}^{2}\mathbf{X}(\varkappa))=\mathbf{T}\,\mathbb{T}_2(\varkappa)$ and ${}^{2}\mathbf{V}(\varkappa)=\mathbf{U}\,\mathbb{T}_2(\varkappa)$, where $\mathbf{T}=[\mathbf{T}_0,\mathbf{T}_1,\mathbf{T}_2]$, $\mathbf{U}=[u_0,u_1,u_2]$, and

$$\mathbb{T}_1(\varkappa)=\begin{bmatrix}1\\ \varkappa^{\varrho}\\ (\varkappa^{\varrho})^2\end{bmatrix},\qquad {}^{\mathrm{R.L}}\mathcal{I}^{\varrho}\mathbb{T}_1(\varkappa)=\begin{bmatrix}\frac{\varkappa^{\varrho}}{\Gamma(\varrho+1)}\\ \frac{\varkappa^{2\,\varrho}\Gamma(\varrho+1)}{\Gamma(2\,\varrho+1)}\\ \frac{\varkappa^{3\,\varrho}\Gamma(2\,\varrho+1)}{\Gamma(3\,\varrho+1)}\end{bmatrix}.$$

Using GFT approach, and solving (46), it follows that

$$\mathbf{T}_0=\Gamma(\varrho)\,\varrho,\quad \mathbf{T}_1=0,\quad \mathbf{T}_2=0,\quad u_0=\Gamma(\varrho)\,\varrho,\quad u_1=1,\quad u_2=0,$$

then

$$\begin{cases} {}^{2}\mathbf{X}(\varkappa)=\varkappa^{\varrho}, \\ {}^{2}\mathbf{V}(\varkappa)=\Gamma(\varrho+1)+\varkappa^{\varrho}. \end{cases} \tag{54}$$

For $d'=3$, from Theorem 3

$$\begin{cases} \min\ J=\displaystyle\int_0^1 \left[\left({}^{1}\mathbb{E}^{\mathbf{X}}(\varkappa)+{}^{2}\mathbf{X}(\varkappa)-\varkappa^{\varrho}\right)^2+\left({}^{1}\mathbb{E}^{\mathbf{V}}(\varkappa)+{}^{2}\,\mathbf{V}(\varkappa)-\varkappa^{\varrho}-\Gamma(\varrho+1)\right)^2\right]\mathrm{d}\varkappa, \\ \text{subject to } 0<\varrho\leq 1, \\ \qquad {}^{\mathrm{C}}\mathcal{D}^{\varrho}_{\varkappa}\left({}^{2}\mathbb{E}^{\mathbf{X}}(\varkappa)+{}^{2}\mathbf{X}(\varkappa)\right)=-\left({}^{2}\mathbb{E}^{\mathbf{X}}(\varkappa)+{}^{2}\mathbf{X}(\varkappa)\right)+\left({}^{2}\mathbb{E}^{\mathbf{V}}(\varkappa)+{}^{2}\mathbf{V}(\varkappa)\right), \\ \qquad {}^{1}\mathbb{E}^{\mathbf{X}}(0)=-{}^{2}\mathbf{X}(0), \end{cases} \tag{55}$$

so

$$\begin{cases} \min\ J = \displaystyle\int_0^1 \left[\left({}^{1}\mathbb{E}^{\mathbf{X}}(\varkappa)\right)^2 + \left({}^{1}\mathbb{E}^{\mathbf{V}}(\varkappa)\right)^2 \right] \mathrm{d}\varkappa, \\ \text{subject to } 0 < \varrho \leq 1, \\ \qquad {}^{\mathrm{C}}\mathcal{D}^{\varrho}_{\varkappa}\, {}^{1}\mathbb{E}^{\mathbf{X}}(\varkappa) = -{}^{1}\mathbb{E}^{\mathbf{X}}(\varkappa) + {}^{1}\mathbb{E}^{\mathbf{V}}(\varkappa), \quad {}^{1}\mathbb{E}^{\mathbf{X}}(0) = 0, \end{cases} \tag{56}$$

so the approximate solution is ${}^{\mathrm{C}}\mathcal{D}^{\varrho}_{\varkappa}({}^{3,2}\mathbb{E}^{\mathbf{X}}(\varkappa)) = \mathbf{T}^{\mathbb{E}^{\mathbf{X}}}\mathbb{T}_3(\varkappa)$, and ${}^{3,2}\mathbb{E}^{\mathbf{V}}(\varkappa) = \mathbf{U}^{\mathbb{E}^{\mathbf{V}}}\mathbb{T}_3(\varkappa)$, where

$$\mathbf{T}^{\mathbb{E}^{\mathbf{X}}} = \left[\mathbf{T}_0^{\mathbb{E}^{\mathbf{X}}}, \mathbf{T}_1^{\mathbb{E}^{\mathbf{X}}}, \mathbf{T}_2^{\mathbb{E}^{\mathbf{X}}}, \mathbf{T}_3^{\mathbb{E}^{\mathbf{X}}}\right], \qquad \mathbf{U}^{\mathbb{E}^{\mathbf{V}}} = \left[u_0^{\mathbb{E}^{\mathbf{V}}}, u_1^{\mathbb{E}^{\mathbf{V}}}, u_2^{\mathbb{E}^{\mathbf{V}}}, u_3^{\mathbb{E}^{\mathbf{V}}}\right],$$

and

$$\mathbb{T}_3(\varkappa) = \begin{bmatrix} 1 \\ \varkappa^{\varrho} \\ (\varkappa^{\varrho})^2 \\ (\varkappa^{\varrho})^3 \end{bmatrix},$$

$${}^{\mathrm{R.L}}\mathcal{I}^{\varrho}\mathbb{T}_3(\varkappa) = \begin{bmatrix} \frac{\varkappa^{\varrho}}{\Gamma(\varrho+1)} \\ \frac{\varkappa^{2\,\varrho}\Gamma(\varrho+1)}{\Gamma(2\,\varrho+1)} \\ \frac{\varkappa^{3\,\varrho}\Gamma(2\,\varrho+1)}{\Gamma(3\,\varrho+1)} \\ \frac{\varkappa^{4\,\varrho}\Gamma(3\,\varrho+1)}{\Gamma(4\,\varrho+1)} \end{bmatrix}.$$

Employing GFT procedure, solving (46), it follows that

$$\mathbf{T}_0^{\mathbb{E}^{\mathbf{X}}} = \mathbf{T}_1^{\mathbb{E}^{\mathbf{X}}} = \mathbf{T}_2^{\mathbb{E}^{\mathbf{X}}} = \mathbf{T}_3^{\mathbb{E}^{\mathbf{X}}} = u_0^{\mathbb{E}^{\mathbf{V}}} = u_1^{\mathbb{E}^{\mathbf{V}}} = u_2^{\mathbb{E}^{\mathbf{V}}} = u_3^{\mathbb{E}^{\mathbf{V}}} = 0,$$

then, we get the approximation for the error ${}^{3,2}\mathbb{E}^{\mathbf{V}}(\varkappa) =^{3,2} \mathbb{E}^{\mathbf{X}}(\varkappa) = 0$ Thus, Eq. (54) represents the exact solution to Problem (50).

8 Conclusion

This paper introduced a robust and computationally efficient framework, the GFT method, for solving multi-dimensional MFOCPs governed by the Caputo derivative and subject to both equality and inequality constraints. The essence of our strategy relies on the combination of a fractional Taylor polynomial base, accurately obtained Riemann–Liouville operational matrix, and Galerkin projection technique. Such a combination results in converting an initial problem to a more manageable algebraic system, which can be handled using conventional nonlinear programming methods. Numerical examples carried out on a number of test problems prove efficiency of our approach. In particular, the GFT method exhibits:

- High Accuracy: Achieving solutions with machine-level precision in specific cases and outperforming existing methods in others.
- Robustness: Reliably handling problems with both state and control inequality constraints through a slack variable formulation.
- Theoretical soundness: Supported by a rigorous a posteriori error estimation framework that allows for iterative refinement without prior knowledge of the exact solution.

Even with its good performance, however, there are some inherent weaknesses in the current formulation of the GFT approach. The speed and accuracy of the method rely, to some extent, on the regularity of the solution being computed; if this solution includes sharp corners or boundary layers, a larger degree of the polynomial will be necessary. Another issue is that the problem size increases with either the dimension of the state vector N or the degree of the polynomial d. Possible avenues for future research, therefore, include:

1. Algorithmic enhancement: Developing an *hp*-adaptive version of the GFT method that dynamically adjusts the polynomial degree (h-refinement) and the fractional order of the basis (p-refinement) to efficiently handle solutions with singularities or steep gradients.
2. Theoretical analysis: A deeper theoretical investigation into the conditioning of the linear systems arising from the GFT discretization, and its dependence on ϱ and d, is necessary to ensure numerical stability for large-scale problems.
3. Broader application: Applying the GFT framework to more complex systems, such as MFOCPs with time-varying delays, fractional partial differential equations, or those involving other fractional operators like the Atangana-Baleanu or tempered fractional derivatives.

On a wider scale, the proposed methodology is a part of the rapidly expanding collection of highly accurate spectral techniques in fractional calculus. Through offering a dedicated approach to handle constrained multi-dimensional MFOCPs, the current study enables precise modeling and optimization of systems characterized by memory and non-locality, which can be applied to areas including viscoelastic control, anomalous diffusion phenomena, and fractional-order circuit analysis. Based on the shortcomings mentioned above, our upcoming research agenda includes:

1. Extending the GFT method to Riemann-Liouville derivatives with proper handling of fractional initial conditions
2. Developing Mittag-Leffler based operational matrices for Atangana-Baleanu derivatives
3. Investigating hp-adaptive strategies for problems with solution singularities or boundary layers
4. Exploring applications to distributed-order and variable-order fractional optimal control problems

Conflict of interest

The authors declare that they have no conflict of interest.

Declarations

Ethical Approval

Not applicable.

Funding

Not applicable.

Availability of data and materials

Not applicable.

References

[1] Nazemi, A., Hosseinpour, S.: A collocation method via block-pulse functions for solving delay fractional optimal control problems. IMA Journal of Mathematical Control and Information 34(4), 1215–1237 (2017). https://doi.org/10.1093/imamci/dnw020

[2] Zhu, Y., Gu, Y., Yan, H.: A numerical method for solving optimal control problems via Legendre polynomials. Engineering Computations 37(8), 2735–2759 (2020). https://doi.org/10.1108/EC-07-2019-0326

[3] Delavarkhalafi, A., Kafash, B.: Application of chebyshev polynomials to derive efficient algorithms for the solution of optimal control problems. Scientia Iranica 19(3), 795–805 (2012). https://doi.org/10.1016/j.scient.2011.06.012

[4] Mirnia, M.K., Yari, A.: Solving optimal control problems by using hermite polynomials. Computational Methods for Differential Equations 8(2), 314–329 (2020). https://doi.org/10.22034/cmde.2020.29747.1433

[5] Peng, H., Li, M.: Solutions of nonlinear constrained optimal control problems using quasilinearization and variational pseudospectral methods. ISA Transactions 62, 177–192 (2016). https://doi.org/10.1016/j.isatra.2016.02.007

[6] Ross, I.M., Gong, Q., Kang, W.: A pseudospectral method for the optimal control of constrained feedback linearizable systems. IEEE Transactions on Automatic Control 51(7), 1115–1129 (2006). https://doi.org/10.1109/TAC.2006.878570

[7] Wang, X., Peng, H., Zhang, S., Chen, B., Zhong, W.: A symplectic pseudospectral method for nonlinear optimal control problems with inequality constraints. ISA Transactions 68, 335–352 (2017). https://doi.org/10.1016/j.isatra.2017.02.018

[8] Khalid, A., Huey, J., Singhose, W., Lawrence, J., Frakes, D.: Human operator performance testing using an input-shaped bridge crane. Journal of Dynamic Systems, Measurement, and Control 128(4), 835–841 (2006). https://doi.org/10.1115/1.2361321

[9] Baleanu, D., Alipour, M., Rostamy, D.: Solving multi-dimensional fractional optimal control problems with inequality constraint by Bernstein polynomials operational matrices. Journal of Vibration and Control 19(16), 2523–2540 (2013). https://doi.org/10.1177/1077546312458308

[10] Ounamane, S., Sadek, L., Abouzaid, B., Sadek, E.M.: Fractional truncated exponential method for linear fractional optimal control problems. Mathematics and Computers in Simulation 232, 408–426 (2025). https://doi.org/10.1016/j.matcom.2025.01.009.

[11] Sadek, L. (2023). Controllability and observability for fractal linear dynamical systems. Journal of Vibration and Control, 29(19-20), 4730-4740. https://doi.org/10.1177/10775463221123354.

[12] Li, H. L., Hu, C., Zhang, L., Jiang, H., & Cao, J. (2022). Complete and finite-time synchronization of fractional-order fuzzy neural networks via nonlinear feedback control. Fuzzy Sets and Systems, 443, 50-69. https://doi.org/10.1016/j.fss.2021.11.004.

[13] Sakthivel, R., Kwon, O. M., Park, M. J., & Sakthivel, R. (2024). Finite-time resilient filtering for discrete-time T–S fuzzy networked control systems with switching communication channels under cyber attacks. IEEE Transactions on Fuzzy Systems, 33(3), 857-868. https://doi.org/10.1109/TFUZZ.2024.3494016.

[14] Ounamane, S., Sadek, L., Abouzaid, B., & Sadek, E. M. (2024). Extended truncated exponential method for solving tempered fractional variational problems. Journal of Vibration and Control, 10775463251320695. https://doi.org/10.1177/10775463251320695.

[15] Sari, M.E.S., Butcher, E.A.: Free vibration analysis of rectangular and annular mindlin plates with undamaged and damaged boundaries by the spectral collocation method. Journal of Vibration and Control 18(11), 1722–1736 (2012). https://doi.org/10.1177/1077546311422242

[16] Marzban, H., Korooeyh, S.S.: Optimal control of linear fractional-order delay systems with a piecewise constant order based on a generalized fractional chebyshev basis. Journal of Vibration and Control 29(17-18), 4257–4274 (2023). https://doi.org/10.1177/10775463221113924.

[17] Heydari, M.H., Razzaghi, M., Avazzadeh, Z.: Orthonormal piecewise bernoulli functions: Application for optimal control problems generated using fractional integro-differential equations. Journal of Vibration and Control 29(5-6), 1164–1175 (2023). https://doi.org/10.1177/10775463211059364

[18] Sadek, L., Ounamane, S., Abouzaid, B., & Sadek, E. M. (2024). The Galerkin Bell method to solve the fractional optimal control problems with inequality constraints. Journal of Computational Science, 77, 102244. https://doi.org/10.1016/j.jocs.2024.102244.

[19] Pakravan, I., Heidari Soureshjani, A., Talebitooti, R., Talebitooti, M.: Haar wavelet technique applied on the functionally graded carbon nanotube reinforced conical shells to study free vibration and buckling behaviors in thermal environments. Journal of Vibration and Control 28(15-16), 1863–1878 (2022). https://doi.org/10.1177/1077546321996931

[20] Kumar, N., Mehra, M.: Generalized fractional-order legendre wavelet method for two dimensional distributed order fractional optimal control problem. Journal of Vibration and Control 30(7-8), 1690–1705 (2024). https://doi.org/10.1177/10775463231169317.

[21] Yüzbaşi, S., Yildirim, G.: Fibonacci wavelets and Galerkin method to investigate fractional optimal control problems with bibliometric analysis. Applied Mathematics and Computation 421, 126956 (2022). https://doi.org/10.1016/j.amc.2022.126956

[22] Sadek, L., Samei, M.E., Hashemi, M.S.: The galerkin mittag-leffler method for solving fractional optimal control problems with inequality constraints. Mathematics

and Computers in Simulation, Volume 240, February 2026, Pages 191-207, (2025). https://doi.org/10.1016/j.matcom.2025.07.018

[23] Yang, Y., Yao, P., Tohidi, E.: A high accurate numerical framework for the solution of the vanishing-delay volterra integro-differential equations via legendre pseudo-spectral element approach. Mathematics and Computers in Simulation, Volume 240, February 2026, Pages 403-422, (2025). https://doi.org/10.1016/j.matcom.2025.07.030.

[24] Yang, Y., Yao, P., Tohidi, E.: Convergence analysis of an efficient multistep pseudospectral continuous galerkin approach for solving volterra integro-differential equations. Applied Mathematics and Computation 494, 129284 (2025). https://doi.org/10.1016/j.amc.2025.129284.

[25] Yang, Y., Tohidi, E., Deng, G.: A high accurate and convergent numerical framework for solving high-order nonlinear volterra integro-differential equations. Journal of Computational and Applied Mathematics 421, 114852 (2023). https://doi.org/10.1016/j.cam.2022.114852.

[26] Yang, Y., Deng, G., Tohidi, E.: High accurate convergent spectral galerkin methods for nonlinear weakly singular volterra integro-differential equations. Computational and Applied Mathematics 40(4), 118 (2021). https://doi.org/10.1007/s40314-021-01469-8

[27] Xiaobing, P., Yang, X., Skandari, M.H.N., Tohidi, E., Shateyi, S.: A new high accurate approximate approach to solve optimal control problems of fractional order via efficient basis functions. Alexandria Engineering Journal 61(8), 5805–5818 (2022). https://doi.org/10.1016/j.aej.2021.11.007

[28] Srivastava, N., Singh, A., Kumar, Y., & Singh, V. K. (2021). Efficient numerical algorithms for Riesz-space fractional partial differential equations based on finite difference/operational matrix. Applied Numerical Mathematics, 161, 244-274. https://doi.org/10.1016/j.apnum.2020.10.032.

[29] Srivastava, N., Singh, A., & Singh, V. K. (2023). Computational algorithm for financial mathematical model based on European option. Mathematical Sciences, 17(4), 467-490. https://doi.org/10.1007/s40096-022-00474-0.

[30] Podlubny, I.: Fractional Differential Equations, to Methods of Their Solution and Some of Their Applications. Fractional Differential Equations: An Introduction to Fractional Derivatives, 340. Academic Press, New York (1998). eBook ISBN: 9780080531984

[31] Sadek, L., Jarad, F., et al.: The general caputo-katugampola fractional derivative and numerical approach for solving the fractional differential equations. Alexandria Engineering Journal 121, 539–557 (2025). https://doi.org/10.1016/j.aej.2025.02.065

[32] Odibat, Z.M., Shawagfeh, N.T.: Generalized taylor's formula. Applied Mathematics and computation 186(1), 286–293 (2007). https://doi.org/10.1016/j.amc.2006.07.102

[33] Xu, X., Xiong, L., Zhou, F.: Solving fractional optimal control problems with inequality constraints by a new kind of chebyshev wavelets method. Journal of Computational Science 54, 101412 (2021). https://doi.org/10.1016/j.jocs.2021.101412

[34] Lotfi, A., Dehghan, M., Yousefi, S.A.: A numerical technique for solving fractional optimal control problems. Computers & Mathematics with Applications 62(3), 1055–1067 (2011). https://doi.org/10.1016/j.camwa.2011.03.044